NUMERICAL MODELLING OF CONTINUOUS TRANSVERSE GRATES FOR HYDRAULIC EFFICIENCY

A THESIS SUBMITTED TO
THE GRADUATE SCHOOL OF NATURAL AND APPLIED SCIENCES
OF
MIDDLE EAST TECHNICAL UNIVERSITY

BY

BERK SEZENÖZ

IN PARTIAL FULLFILLMENT OF THE REQUIREMENTS
FOR
THE DEGREE OF MASTER OF SCIENCE
IN
CIVIL ENGINEERING

OCTOBER 2014

Approval of the thesis:

NUMERICAL MODELLING OF CONTINUOUS TRANSVERSE GRATES FOR HYDRAULIC EFFICIENCY

submitted by **BERK SEZENÖZ** in partial fulfillment of the requirements for the **degree of Master Science in Civil Engineering Department, Middle East Technical University** by,

Prof. Dr. Canan Özgen
Dean, Graduate School of **Natural and Applied Sciences** _____

Prof. Dr. Ahmet Cevdet Yalçıner
Head of Department, **Civil Engineering** _____

Assoc. Prof. Dr. Şahnaz Tiğrek
Supervisor, **Civil Engineering Dept., METU** _____

Examining Committee Members

Prof. Dr. A. Burcu Altan Sakarya
Civil Engineering Dept., METU _____

Assoc. Prof. Dr. Şahnaz Tiğrek
Civil Engineering Dept., METU _____

Assoc. Prof. Dr. Mete Köken
Civil Engineering Dept., METU _____

Assoc. Prof. Dr. D.Funda Kurtuluş Bozdemir
Aerospace Engineering Dept., METU _____

Dr. Nihal Yılmaz
Gazi University,DLTM-Teknopark _____

Date: 20 October 2014

I hereby declare that all information in this document has been obtained and presented in accordance with academic rules and ethical conduct. I also declare that, as required by these rules and conduct, I have fully cited and referenced all material and results that are not original to this work.

Name, Last name: Berk SEZENÖZ

Signature :

ABSTRACT

NUMERICAL MODELLING OF CONTINUOUS TRANSVERSE GRATES FOR HYDRAULIC EFFICIENCY

Sezenöz, Berk

M.S., Department of Civil Engineering

Supervisor: Assoc. Prof. Dr. Şahnaz Tiğrek

October 2014, 64 Pages

In this study, numerical analyses of newly proposed grated inlet system for small roads are carried out. The model is based on a setup constructed in Hydromechanics Laboratory of METU. The physical model which is a rectangular channel of 0.9m width acts as a small road and continuous transverse grate system is installed as an inlet structure. The physical conditions were modeled by using Flow 3D software. The rates of the intercepted flows are measured and compared with the results of experimental data collected previously. In addition, channel capacity of the system has increased in numerical model in order to see behavior of the system with the higher amounts of flow rates. The efficiencies of continuous transverse grate are calculated with the various amounts of flow rates and their relations with total flow rates and Froude numbers are demonstrated.

Keywords: Intercepted flow, Bypass flow, Grate Capacity, Grate Efficiency, Continuous Transverse Channel, Grate Inlets

ÖZ

SÜREKLİ ENLEMESİNE OLAN IZGARALARIN VERİMLİLİKLERİ İÇİN SAYISAL MODELLEME

Sezenöz, Berk
Yüksek Lisans, İnşaat Mühendisliği Bölümü
Tez Yöneticisi: Doç. Dr. Şahnaz Tiğrek

Ekim 2014, 64 Sayfa

Bu tez çalışmasında küçük yollar için yeni yöntem olarak önerilen ızgara drenaj sistemleri bilgisayar ortamında sayısal çözümleme yöntemiyle incelenmiştir. Model daha önce ODTÜ Hidromekanik laboratuarında tasarlanan ve inşa edilen düzeneğe dayanmaktadır. Dikdörtgen kanal şeklinde düzenlenen model küçük bir yol platformu vazifesi görmekte olup genişliği 0.9 metre olarak alınmıştır ve bu platform ızgaralı drenaj sistemine bağlanmıştır. Fiziksel koşullar Flow 3D programı ile modellenmiştir. Bilgisayar modelinde ızgaradan geçen akım miktarları hesaplanmış ve bu sonuçlar daha önce gerçekleştirilen deney sonuçları ile karşılaştırılmıştır. Daha önce yapılan çalışmalara ek olarak bu modelde kanal kapasitesi arttırılıp düzeneğe daha yüksek debide akımlar verilmiş ve yüksek akımlar karşısında ızgara sisteminin nasıl davranış sergileyeceği izlenmiştir. Birçok debi için ızgara verimlilikleri hesaplanmış ve bunların sisteme verilen toplam debi ve Froude sayısı ile olan ilişkileri incelenmiştir.

Anahtar Kelimeler: Tutulan Akım, Geçen Akım, Izgara Kapasitesi, Izgara Verimliliği, Sürekli Devam eden Izgara Sistemi, Izgaralı Drenaj Sistemi

To My Family & Friends

ACKNOWLEDGEMENTS

First of all, I wish to express my deepest gratitude to my supervisor Assoc. Prof. Dr. Şahnaz Tiğrek for her patience, guidance, instructions and suggestions in every stage of this study.

I want to thank Ozkar Construction Company and my workmates for showing me tolerance in this thesis study.

I also want to special thanks to my friend Eray Usta. He helped me every step of this thesis and always encourage and motivate me to complete this thesis.

My deepest gratitude goes to my parents and my family. They always support and help me in every step of my life and I really appreciate that I have a great family and without their support this thesis would not have been completed.

TABLE OF CONTENTS

LIST OF TABLES

TABLES

LIST OF FIGURES

FIGURES

LIST OF SYMBOLS AND ABBREVATION

S= Slope

Q_T= Total flow

E= Grate Efficiency

L= Length

q= Unit Discharge

e= Unit Efficiency

Q_i= Intercepted Flow

Q_b= Bypass Flow

E_s= Specific Energy

CFD= Computational Fluid dynamics

VOF= Volume of Fluid

F= Fraction Variable

A= Area

R= Hydraulic Radius

n= Manning Roughness Coefficient

y= Depth of Water

g= Gravity

Fr= Froude Number

V_{avg}= Average Velocity

y_n= Uniform Depth

CHAPTER 1

INTRODUCTION

1.1 General: Problem Definition

Prevention or control of flood due to surface runoff becomes very common issue in impervious area of the urban environment such as highways, squares, airports, parks and paved areas. Surface runoff can be captured with accurate design systems. However, the design process is sophisticated, since the problem is both a part of hydrology and hydraulics. The designer should consider several parameters. Flood can occur due to inadequate capacity of the storm collection systems or high intensity rainfall. If the surface run off cannot be fully captured by the drainage system, by-pass flow may create hazardous results.

1.2 Scope of the Study

In this technical study, efficiency of the continuous grate drainage system will be investigated by using numerical approach with a computational fluid dynamics. The platform which was built in the METU Hydromechanics laboratory for the thesis of Calibration of a Grate on a Sloping Channel by Sipahi (2006) will be simulated by using commercial software, namely Flow 3D, and efficiency of the system will be analyzed for range of flow rates. The results will be compared with available studies (Sipahi, 2006) and Gomez and Russo, 2009).

CHAPTER 2

REVIEW OF EXPERIMENTAL STUDIES ON GRATE EFFICIENCY

2.1 General

Drainage water is generally collected by a system consist of inlets and pipes. In conventional types of storm drainage systems, inlets are located near the curbs (Figure 2.1 and 2.2) (Bengtson, 2010) to collect water by using gradients to inlets near the curbs. If there is not well defined thalweg or proper gradients that direct the flow through the inlets, the conventional system can be defined as ineffective. Instead of using conventional system, to place continuous grates perpendicular to the flow direction may help to collect water more efficiently. Thus it reduces the risk of by-passing flood flow.

Continuous grate drainage system (Figure 2.3 and 2.4) (Bengtson, 2010) is composed of grate and the channel beneath it. Since those elements are members of the whole, they should be investigated separately and jointly. However, in this study only efficiency of the grate is investigated and the under channel capacity is taken as considerably large in order to eliminate the effect of the inadequate inlet capacity and rebounding flow.

Figure 2.1 Example of Curb Inlet

Figure 2.2 Example of Curb Inlet with grate

Figure 2.3 Continuous Grate Inlet in Site

Figure 2.4 Continuous Grate Inlet

2.2 Review of the Laboratory Studies

Since design of continuous grated inlets and the efficiency of the system have not been studied detailed yet, two laboratory studies are lightened our process of numerical setup. Calibrations of a grate on a sloping channel by Sipahi (2006) which will be called as, Experiment 1, and hydraulic efficiency of continuous transverse grates for paved areas by Gomez and Russo (2009), which will be called as Experiment 2, are the two real case studies of which results and setups form the foundation of our study.

2.2.1 Experiment Study 1

This experiment setup was built in METU Hydromechanics Laboratory. The system is built on a steel channel and fiber glass platform implanted on it. The width of the steel channel is 1.00 m. The width of the fiber glass channel is designed as 0.90 m, having 5 cm spacing from both sides. The height of the implanted channel is 0.45 m. 0.10 m deep upper portion having a slab constituting the channel as shown in Figure 2.5(All dimensions are in m.).

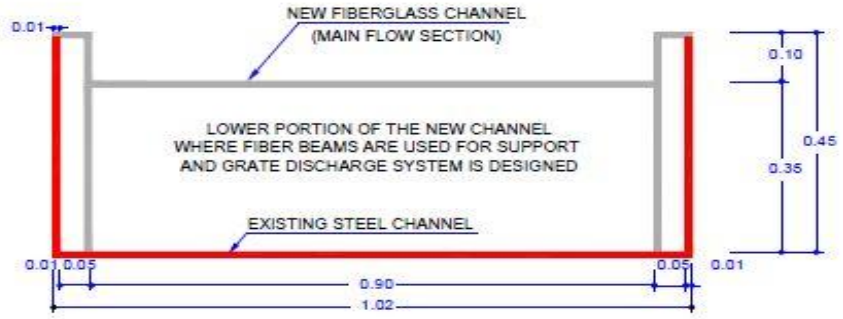

Figure 2.5 Experiment 1 Channel Section (after Sipahi, 2006)

The setup was constructed to measure more than one grate efficiency. However, in the experiment one grate was used because of availability of the laboratory conditions. The location of the first grate is designed to be towards the end of the channel in order to satisfy steady state flow conditions as much as possible. At the location of first grate, the fiber glass support beams form a reservoir for the water to be taken from the first grate. From the reservoir under the grate, intercepted water is carried with a rectangular discharge channel to the reservoir pool. The remaining bypassed flow on the upper channel reaches to the location of second grate. In the same way second grate and third grate by passed flow remains in the upper channel and collected in separate reservoir pool for flow measurement. Figure 2.6(All dimensions are in m.) shows Top view of the experiment setup.

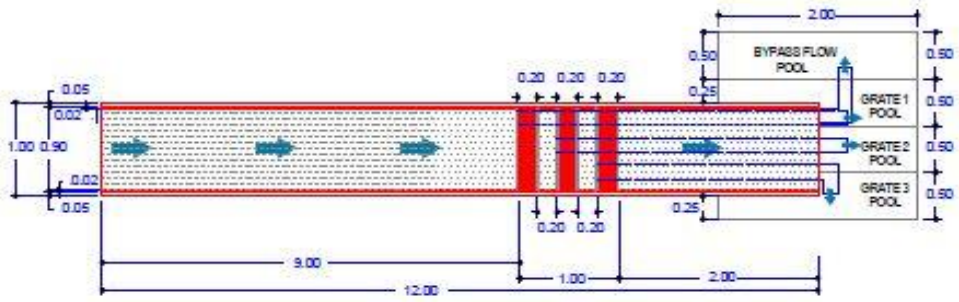

Figure 2.6 Experiment 1 Top Views (after Sipahi, 2006)

Grate details and dimension of the grate is shown in Figure 2.7(All dimensions are in m.);

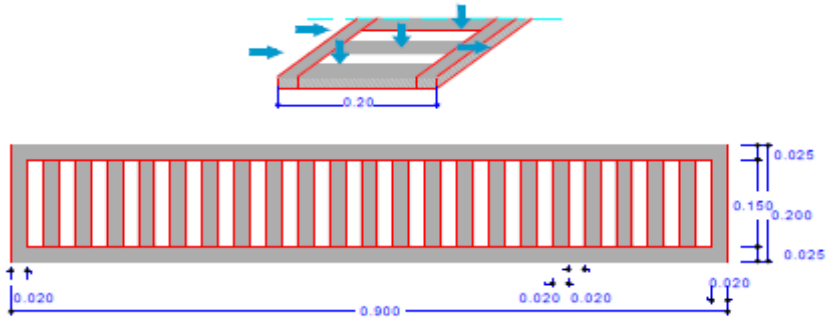

Figure 2.7 Grate Details (Sipahi, 2006)

In the laboratory experiment of Sipahi (2006), 1st grate of the system at 9th meter was used as an inlet of the system. However, grate 2 and 3 were covered with a fiber glass material. Although, Sipahi (2006) worked with different longitudunal slopes, in our computational model only slope of 1% was investigated. Sipahi's (2006) results belong to slope of 1% are given in Table 2.1 and Figure 2.8 and will be compared with computational model in results and discussion chapter.

Table 2.1 Results of the Sipahi (2006)
Experimental Study for Slope 0.01

Total Flow (10^{-3}m3/s)	Intercepted Flow (10^{-3}m3/s)	By-Pass Flow (10^{-3}m3/s)
0.41	0.23	0.18
1.10	0.74	0.36
1.61	1.19	0.43
2.84	2.34	0.50
4.27	3.76	0.51

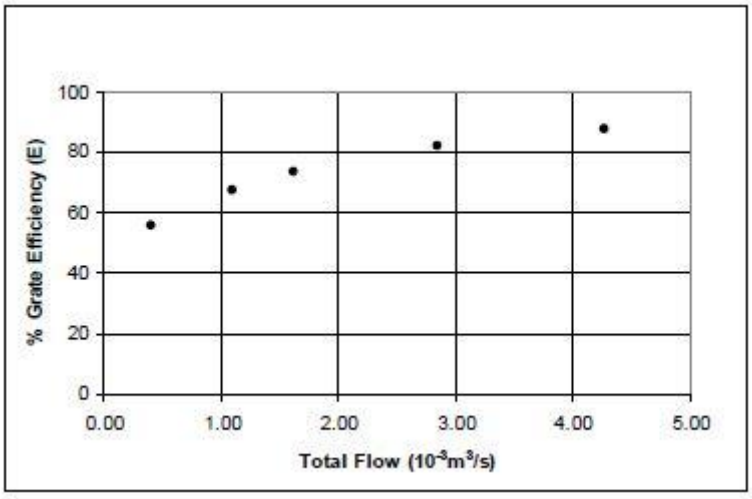

Figure 2.8 Grate Efficiency versus Total Flow(Sipahi, 2006)

2.2.2 Experiment Study 2

Different types of hydraulic structures were tested in the laboratory of the University of Catalonia Hydraulic Department. Tests were made in a 1:1 scale on a rectangular testing area that is 1.5 m wide and 5.5 m long which is shown in Figure 2.9. The platform is able to simulate lanes with transversal slope up to 4% and longitudinal slope up to 14%. It is possible to test surface drainage structures and study their hydraulic capacity for a large set of flows 0–200 l/s. Pump systems discharge the flow up to a tank placed approximately 15 m above the platform. A motorized slide

valve regulates the flow discharged to the model. Discharge measurement is done by an electromagnetic flow meter with an accuracy of 1 l/ s. The intercepted discharge by the inlet is conveyed to a V-notch triangular weir and the flow measurement is carried out through a limn meter with an accuracy of 0.1 mm.

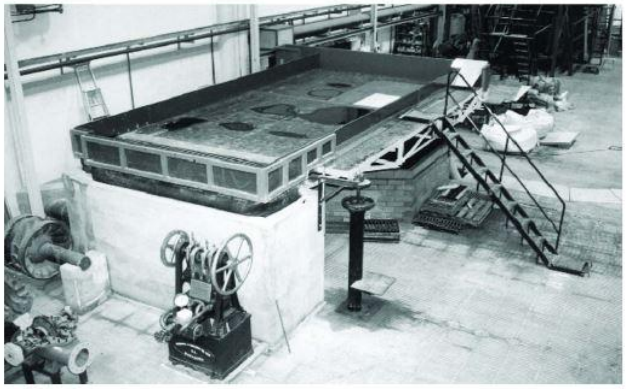

Figure 2.9 Platform of the model (Gomez and Russo, 2009)

Four different types of grates (Figure 2.10) were used in this experiment, however grate type 3 is very similar to Sipahi's (2006) study so that results obtained from grates 3 is taken into consideration for our numerical study. Geometric parameters of grates are shown below Table 2.2.

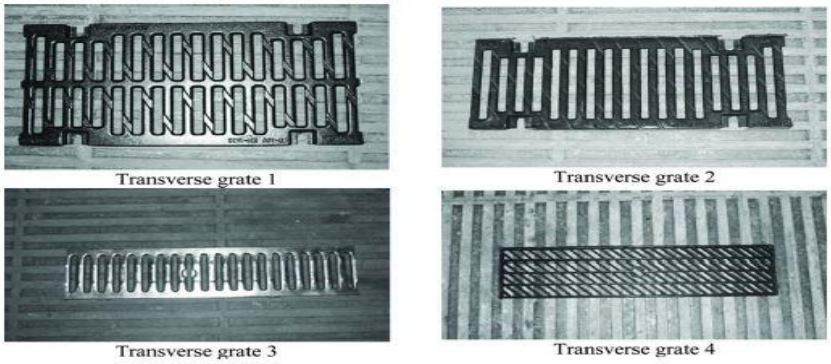

Figure 2.10 Experiment 2 Types of Grates (Gomez and Russo, 2009)

Table 2.2 Grate Geometrical Parameters (Gomez and Russo (2009))

Transverse grate type	Width (cm)	Length (cm)	Efective Length (cm)	Total Area (cm^2)
1	100	30.2	25.0	3.02
2	100	19.5	15.0	1.95
3	100	12.4	10.4	1.24
4	100	12.4	12.0	1.24

Following unit flows are tested in the experiment 6.7, 16.7, 33.3, 50, and 66.7 l/s/m. The upper values allow one to represent the real flows circulating on paved areas in the case of medium or heavy rain falls. Following longitudinal slopes 0, 0.5, 1, 2, 4, 6, 8, and 10% were tested. As mentioned in subsection 2.2.1, experimental results using bottom slope of S=1% is taken into consideration and the results of which are shown below Figure 2.11. Comparison of the results with computational model will be evaluated at the results and discussion chapter.

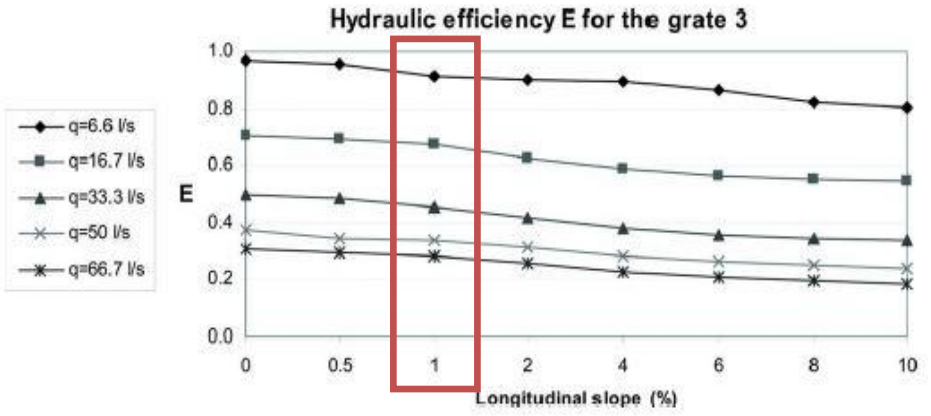

Figure 2.11 Efficiency vs. Longitudinal Slope for Grate Type 3 (Gomez and Russo (2009))

2.3 Comparison of the Results of Experiment 1 and Experiment 2

Combination of results of Sipahi (2006) and Gomez and Russo (2009) are illustrated Figure 2.12.

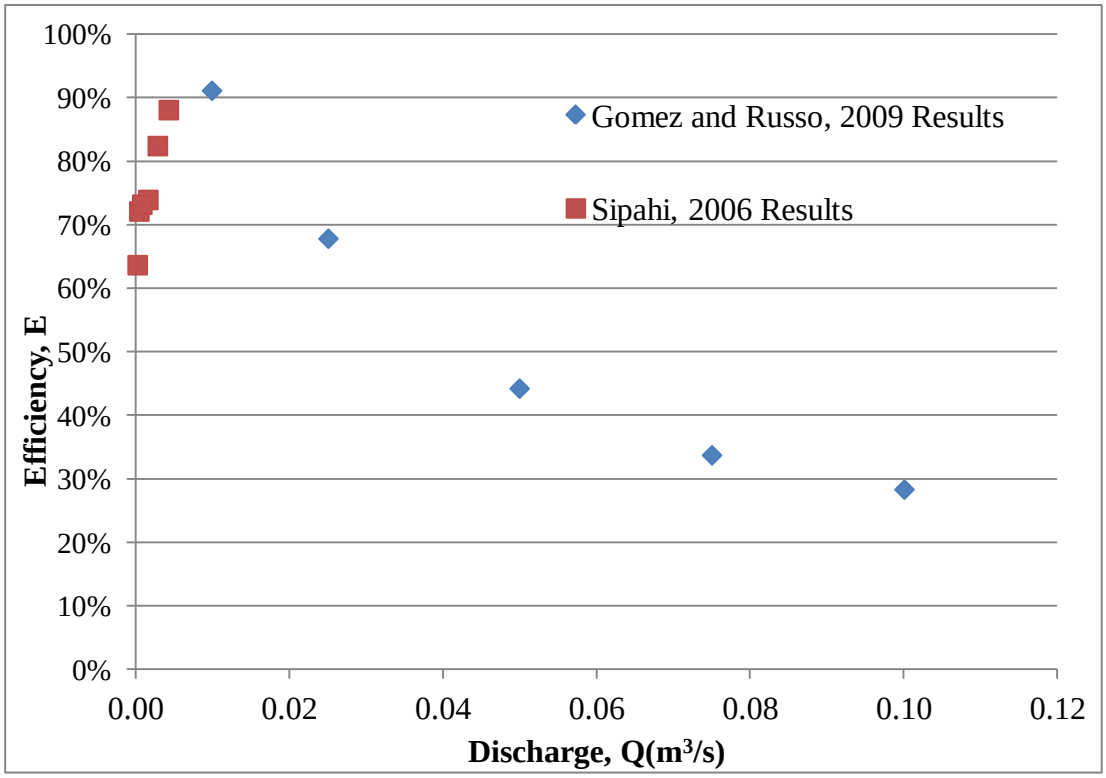

Figure 2.12 Efficiency versus Total Flow Graph for Studies of Sipahi (2006) and Gomez and Russo (2009) for S=0.01

As seen in Figure 2.12, efficiencies of grate system increase with increasing flow rates up to a level and then it start to decrease. In other words, system can be divided into two parts and both parts should be investigated. Main reason to carry out this thesis study is to investigate two parts of the system and compare the results with recent studies.

CHAPTER 3

THEROTICAL BACKGROUND

3.1 General Information

Storm water runoff creates numerous safety problems in the urban areas. Those problems can be magnified because of the increases in traffic and pedestrian density. Storm water inlets are provided to collect storm water from paved areas. It is important to have sufficient capacity of collecting system after intercepting surface runoff otherwise drainage system can be defined as inefficient. However, there are too many parameters that effects design stage of the drainage system. When selecting and locating inlets consideration shall be hydraulic efficiency, vehicle, pedestrian and bicycle safety, debris collection and maintenance problems. Four types of inlets may be utilized for pavement drainage (HEC 22, 1991);

- Grate Inlet
- Curb Inlet
- Slotted Inlet
- Combined Inlet (Curb and Grate)

Since this study is focusing on grate inlets, the emphasize should be given on them. Grates are effective in intercepting gutter flows and they also provide access for maintenance. Type and shape of the grates should be arranged by considering duration of flow, path of flow, surface slope, surface texture and rainfall density. Those parameters should be investigated in detail in order to take precautions following problems and disadvantages of the grate inlet system;

- The hydraulic regime of the operation of the structure
- Geometry of the grating
- Accumulation of debris at the gratings

This technical study is focusing on the efficiency of the transverse grate with various flow rates at the constant slope of S=1% , the other parameters such as type of grates, number of grate bars and void area of the grate, etc. and their effects of efficiency may be investigated in the future studies.

3.2 Methodology

3.2.1 Hydraulic Efficiency of Grated Structures

Hydraulic efficiency of inlets can be described as ratio of the intercepted flow by the grate to total flow which is the sum of the intercepted flow and by pass flow passing through the grates. This description is valid if there is no surcharge effect in channel.

$$E=Q_i/Q_t \quad (3.1)$$

$$Q_t=Q_i+Q_b \quad (3.2)$$

Where E is the efficiency, Q_i is total intercepted flow rate, Q_t is total flow approaching to inlet and Q_b is the by-pass flow. Efficiency is affected many hydraulic parameters such as longitudinal slope of the paved area, transversal slope of the paved area, roughness (n), geometry of paved area and clogging factors. Total flow rate is another factor affecting the efficiency. Considering flow it is expected that, efficiency will decrease when flow rate increases. This statement can be valid generally; however this study will give unexpected results which will be observed from the next chapter. In addition to hydraulic parameters, geometric parameters of grates are the other concerns that need to be investigated when calculating efficiency. Type of grates, distance between parallel bars, and arraying style of the bars can be counted as the main geometric parameters.

Gomez and Russo (2009) used unit discharge to estimate efficiency of the continuous grate system.

$$e=q_i/q_t \quad (3.3)$$

Where e is the efficiency per meter of grates, q_i intercepted flow rate per unit width and q_t is total flow rate per unit width.

3.2.2 Theoretical Approach of Grate Inlets

Hydraulics of grated inlets can be defined as spatially varied flow in which discharge varies in the direction of flow. According to Chow (1959) this varied flow may be treated as flow diversion where the diverted water does not affect the energy heads.

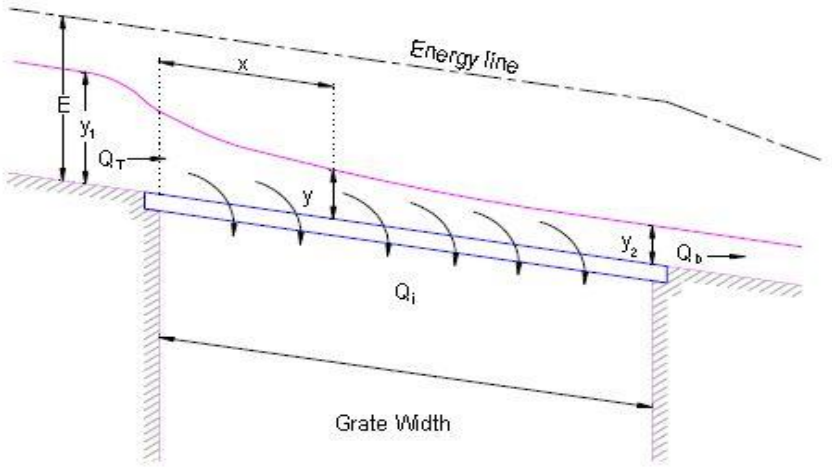

Figure 3.1 Spatially Varied Flow with Decreasing Flow Rate (Chow , 1959, reproduced by Sipahi (2006))

The specific energy, E_s is described as follow,

$$E_s = y + Q^2/(2gb^2y^2) \quad (3.4)$$

Where E_s is the specific energy, y is flow depth, g is gravity and Q is volumetric discharge and b is the width of channel.

From equation (3.4), discharge can be written as;

$$Q = by(2g(E_s - y))^{0.5} \quad (3.5)$$

From equation (3.5), total and by-pass flow can be written as;

$$Q_T = by_1(2g(E_s - y_1))^{0.5} \quad (3.6)$$

$$Q_b = by_2(2g(E_s - y_2))^{0.5} \quad (3.7)$$

So we can rewrite intercepted flow as;

$$Q_i = Q_T - Q_b \quad (3.8)$$

Motskow (1957) proved that efficiency values experimentally increase as longitudinal slope approaches to horizontal slope. He also proved that this is valid only if grates bars are parallel to direction of flow. However, in real cases horizontal slopes may create clogging problems and debris accumulation so this will bring another problem in the design stage.

CHAPTER 4

FLOW 3D AS A TOOL FOR NUMERICAL SOLUTION

4.1 General Information

Flow 3D computational software which can be counted as one of the famous tool for creating CFD (Computational Fluid Dynamics) Model. CFD is the science about calculation of fluid flow and related variables using a computer. Usually fluid body is divided into cells or elements forming grid. Then equations for unknown variables are solved for each cell. This science is extremely developed in recent years with the development of computer technology. CFD modeling allows us to solve more complex and sophisticated problems in considerably short time and economical way when it is compared to traditional physical models. Flow 3D is a powerful software that solve fluid motions, phase changes (boiling, melting, cavitations, solidification etc.), multi phase flow (air entrainment sediment flow etc.), solid motions, solid stress and deformation (tank failure, weir buckling, sediment erosion etc.) and thermal transportation. Flow 3D software solves the Navier-Stoke system of equations in 3D to simulate the flow of fluid.

4.2 Modeling of the Problem and Boundary Conditions

In order to create a new simulation in the software you can use a civil drawings software to build a solid body. After drawing the entire model as a solid body you can import it to flow 3D software. It is also possible do embed all of the topographic properties to flow 3D simulation. You can build primitive shape and body system by Flow 3D, however complex system have to be drawn by using civil drawings software. In one simulation you can add more than one subcomponent. In addition, the software allows the users to use more than one subcomponent and assemble all the subcomponents to create the model.

Boundary conditions are the most important part of the modeling. In this software you can give different boundary conditions to every single mesh block system. You can find 10 boundary condition options in Flow 3D software. (Figure 4.1)

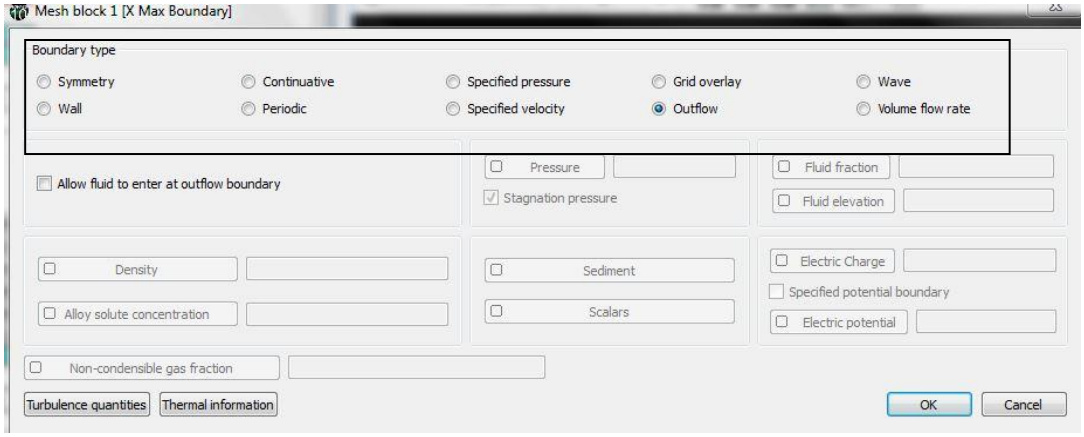

Figure 4.1 Boundary Types in Flow 3D

4.3 Volume of Fluid Method

Flow 3D software use VOF (Volume of Fluid) method in calculations. The trademark of TruVOF is enhanced for that reason. To obtain accurate free surface for VOF method necessary three requirements are provided in the software;

1. Fraction variable F is calculated for each cells. If F=1, it indicates the cells are fully filled with fluid, if F=0 it indicates that cell is empty.
2. To obtain accurate free surface is very important. Since, fraction factor F is calculated for every cells it is possible to obtain free surface accurately.
3. Boundary conditions are the other important concern for VOF method. As it is mentioned before there are 10 boundary conditions in the software and you can choose appropriate boundary condition with the several choices.

4.4 Grid Domain

Flow 3D software is dealing with the orthogonal meshes to define control volumes. The program generally use uniform meshes and calculate the Navier-Stoke equations at every mesh center. It also allows to different types of mesh blocks in one model (Figure 4.2 (Flow 3D, v10.1 User Manuel, (2012).). In other words, you can add more than one mesh block system according to the study. If you need detail analyses in specific area you can decrease the dimensions of the meshes to obtain more cells. In addition, you can assign cell dimension or cell numbers into the system. The gridlines between different mesh blocks should intersect for accurate calculation and 2:1 rules have to apply in the studies (Figure 4.3(Flow 3D Lecture Notes, 2012). However, assigning too much cells will extent your computation progress. Since calculations are done for every cells, increasing amount of cells will increase time of computation. So, optimum amount of cells should be assigned.

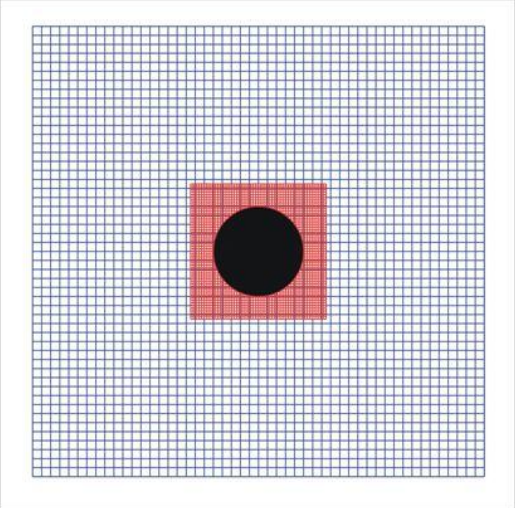

Figure 4.2 Example of Multiple Mesh Block

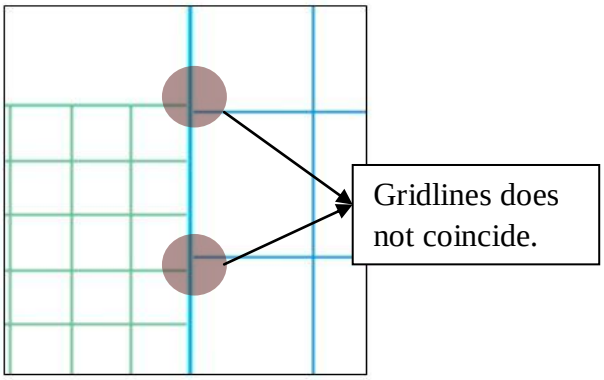

Figure 4.3a Wrong Grid Placement

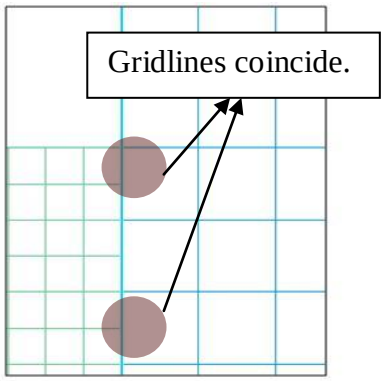

Figure 4.3b Accurate Grid Placement

For the beginning, optimum amount of cells can be obtained by FAVOR option. Since the cells are orthogonal, you have to obtain optimum size of cells to generate system one of the same with the real case. If cell sizes are not optimum, geometry problems will be occurred (Figure 4.4 Flow 3D, Advanced Hydraulics Training, (2012)). To avoid those problems, FAVOR option help users to obtain accurate geometric shapes.

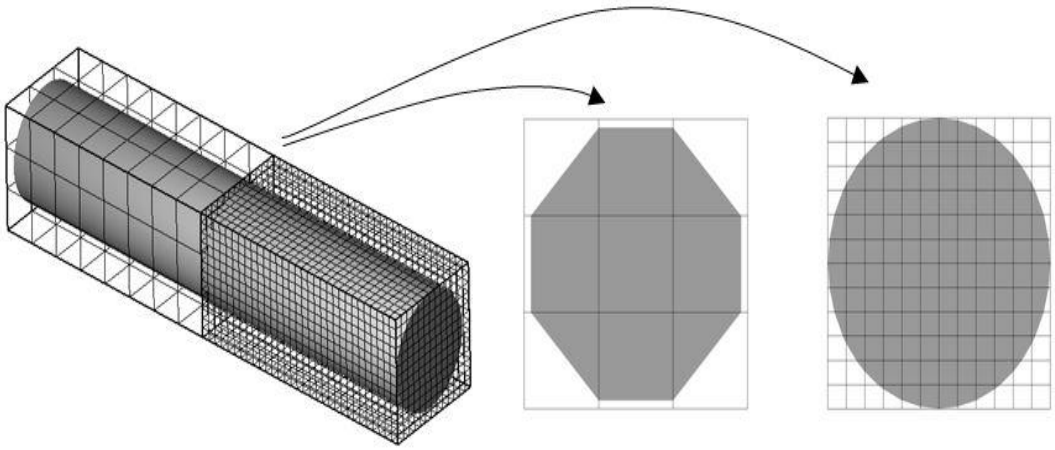

Figure 4.4 Favor Option with Different Cell Size

CHAPTER 5

MODELLING PROCESS AND RESULTS

5.1 General Information

In this chapter intercepted flow through the grates will be investigated and efficiency of the grates with different flow rates will be calculated. Physical Model which was built by Sipahi (2006) will be simulated by using Flow 3D software and also Gomez and Russo (2009) physical model will be taken into consideration for higher discharge quantities.

5.2 Physical Model

System which was built by Sipahi, (2006) was taken as a physical model in this study. As mentioned in chapter 2, the model includes a platform and a channel passing beneath it. The platform has length 12 meter with a continuous grate at the 9^{th} meter. Gomes and Russo (2009) model was built in a same manner with a 5.5 meter platform in length and 1.5 meter in width. The main difference between two laboratory studies is placement of grate. This means that, Sipahi, (2006) used continuous grate which covers the entire platform and there is no space between the side walls of the platform and main channel, while Gomez and Russo (2009) used continuous grate with a space between side walls and main channel which let by-pass flow on the spaces between end of grates and side walls. The other important point is the range of the flow rates. Since, Sipahi (2006) flow rates amount is considerably less than Gomez and Russo (2009) combination of both laboratory studies will be taken into consideration.

As it is shown in Figure 2.5 the platform was made by fiber glass with a width of 90 cm and height of 10 cm. The system consists of 3 continuous grates and 3 channel under the grates. Channels are connected to the pool system to calculate total volume of the water. However, the study in laboratory was carried by single grate system. The other grates were covered and not taken into consideration. In this study some rectifications are done to decrease total calculation duration. Thickness of the fiberglass platform is 0.01 m in real cases but it is taken as 0.5 m to increase size of the cells in order to decrease number of cells to reach optimum mesh size. Since, width and length of the platform were taken as original value; this arrangement will not affect the results of the system. In simulated model, intercepted flow is directly taken to channel beneath the main channel instead of channel beneath to grate to increase the capacity of system. Since, Sipahi (2006) was dealing with lower amounts of volumetric flow rates, limited capacity of the channel under grate was not considered, but in this study volumetric flow rates considerably increased so that channel capacity under the grate remain incapable. In order to increase capacity without changing the system intercepted flow directly release to channel under grate.

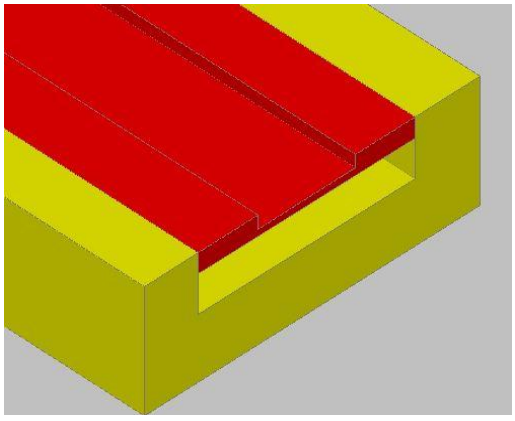

Figure 5.1a Model(Cross Section of the Model)

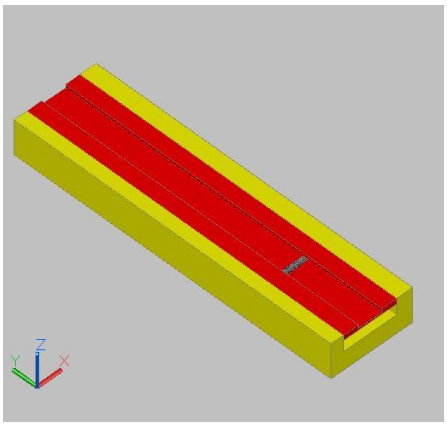

Figure 5.1b Model (Top view of the Model)

5.3 Development of Computer Model

5.3.1 Grate Location and Dimensions

The physical model is simulated with some minor edits in Flow 3D tool. At first, solid body is created in AutoCAD format (Figure 5.1). At the 9th meter continuous grate was embedded on the platform. Longitudinal slope is taken as %1. The grate is taken as it is in laboratory model. 3D view and dimensions of the grate is indicated in the Figures 5.2 and 5.3(all dimensions in meter).

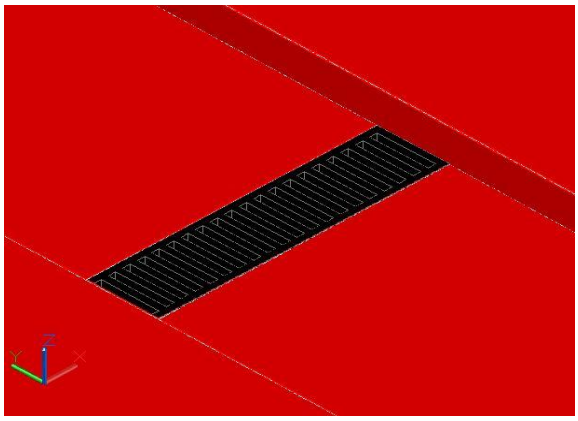

Figure 5.2 3D View of the Continuous Grate

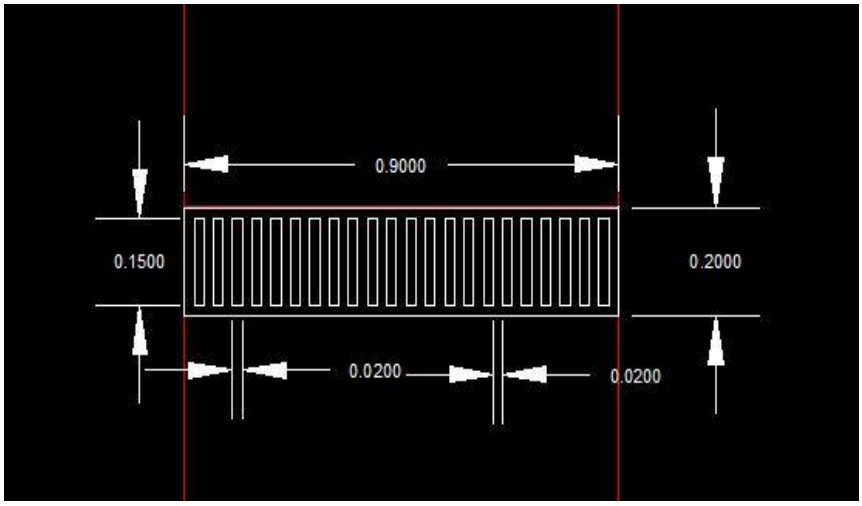

Figure 5.3 Dimensions of the Grate in the Model

5.3.2 Modifications on the Solid Body

In order to ease process of developing model and calculations, some rectifications had been made on the solid system. As it is illustrated in Figure 5.5 blocks were added on the back of the platform. Back wall was used for a cover to close the hole of the channel under the waterline platform and two side walls was added to solid body to let the flow pass through its original path. Since flow was given to system at the beginning of the platform, it is necessary to close this area not to take any extra flow from the source of the system (Figure 5.4). Although, it can be considered that this arrangement was elongated the length of the platform, this will not affect the results of the system but it gave opportunity to assign volumetric flow rate.

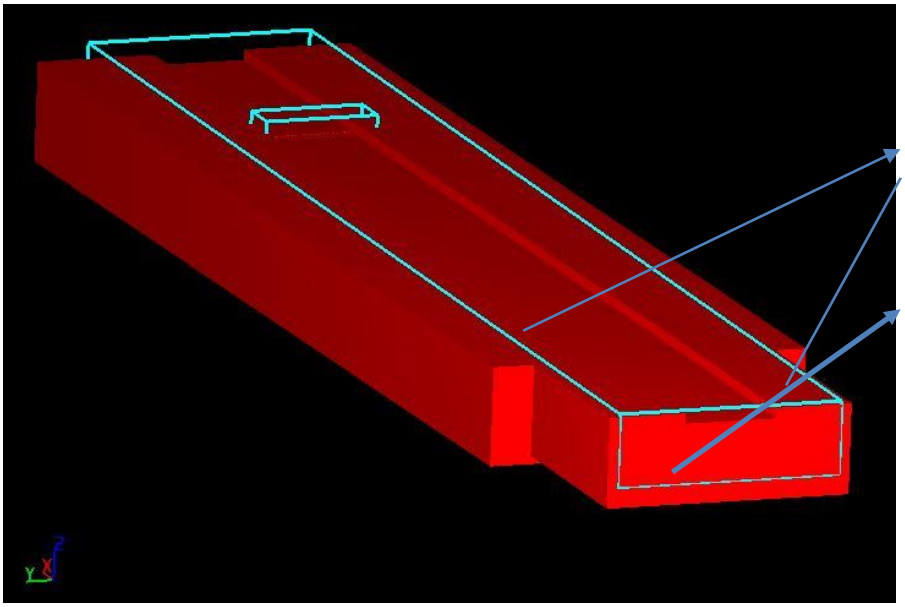

Figure 5.4 View of the Simulated Model

5.3.3 Meshing Process

One mesh block with size cell of 0.04 m was considered for the first approach. However, grate dimensions are too small to create the same geometry (grate thickness is 2 cm and offset distance between grate bars 2 cm) in the software by using FAVOR option of software. As it was mentioned in chapter 3 FAVOR option give opportunity to reach optimum mesh number before any calculation. Shape of the system after FAVOR option is depicted on the Figure 5.5.

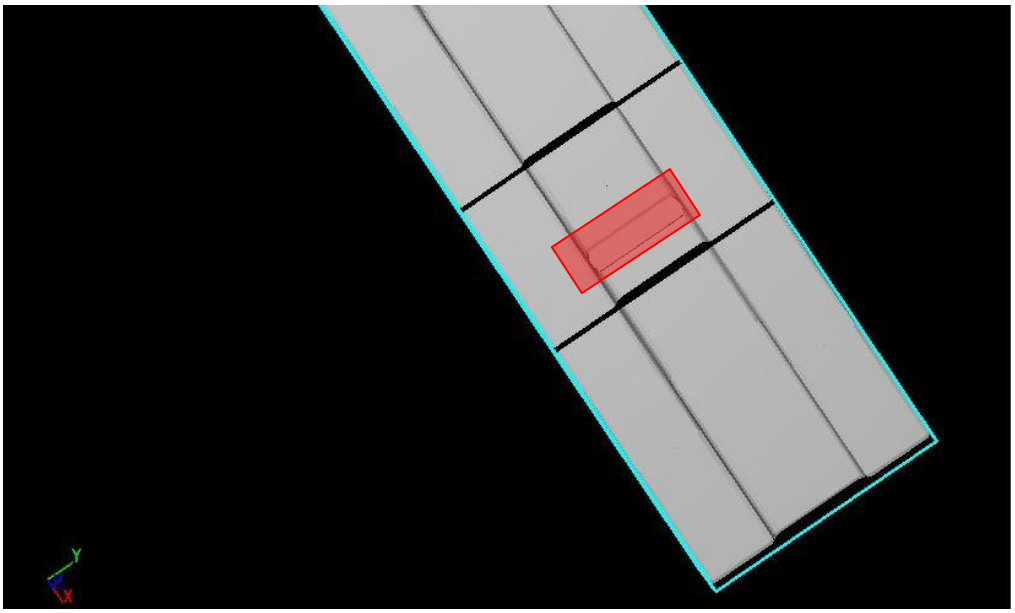

Figure 5.5 Shape of the Model after First Meshing

As it is emphasized by red color in Figure 5.5 grate area cannot be defined by using mesh block with size 0.04 m. For this reason, it is considered that one mesh block with small size will increase the number of the cell and duration of calculation so two mesh blocks were used in the 2nd trial. First mesh block with size 0.04 m and second mesh block with size 0.02 m were considered. Second mesh block was defined on grated area while first mesh block was defined for remaining part. However, this system was not sufficient to obtain the same grate geometry as it is on the model in the laboratory (Figure 5.6).

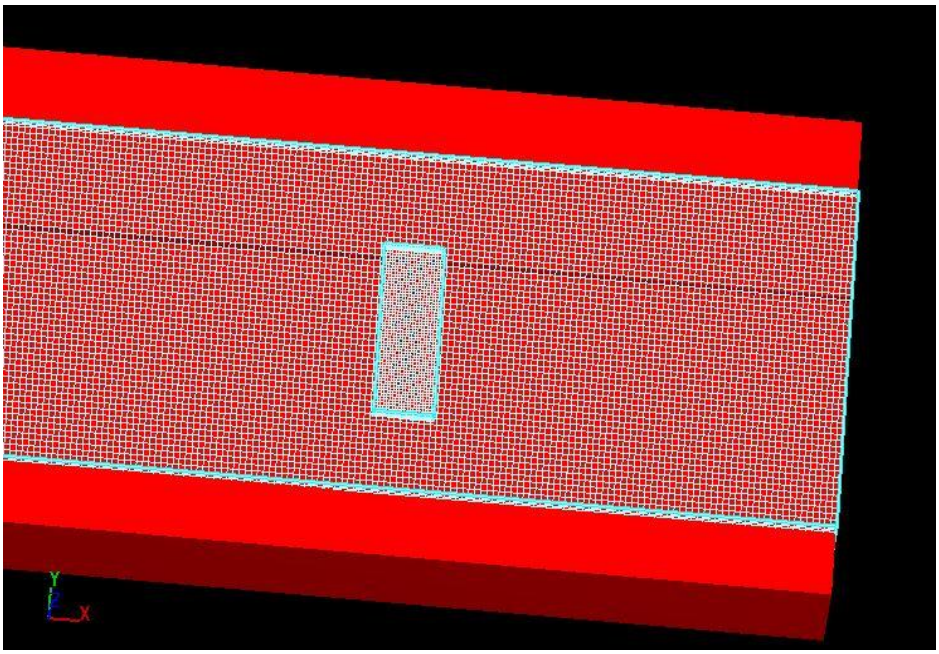

Figure 5.6 Meshing Grids of Second Trial

In the 3rd trial, mesh block with sizes 0.02 m and 0.01 m were used. Since, 2:1 ratio is very important for accurate calculation in flow 3D as it is mentioned in chapter 4, the dimensions of the cells were arranged by considering this rule. The other reason to decrease size of cell 0.04m to 0.02m is the depth of the water. Since we are dealing with small amount of volumetric flow rates (0.1, 0.075, 0.5, 0.025, 0.01 and 0.00427 m^3/s) the depths of the volumetric flow are considerably small (depth of flow will be given in next chapter). In the 4th trial, mesh block with sizes 0.02 m and 0.005 m were used. Finally, it was observed that the duration of the final trial is very long (96 hours) and the results of the mesh block with sizes 0.02 m and 0.01 m are more accurate with the experiment of Sipahi (2006). Hence, mesh block system with 0.02 m and 0.01 m was accepted as the optimum mesh size. Geometry of the model after last arrangements is shown in the Figure 5.7. Finally, 2.695.000 and 308.000 cells were calculated for the 1st and 2nd mesh block respectively. Total numbers of 3.003.000 cells were taken into consideration in this study results of them will be given in the next chapter.

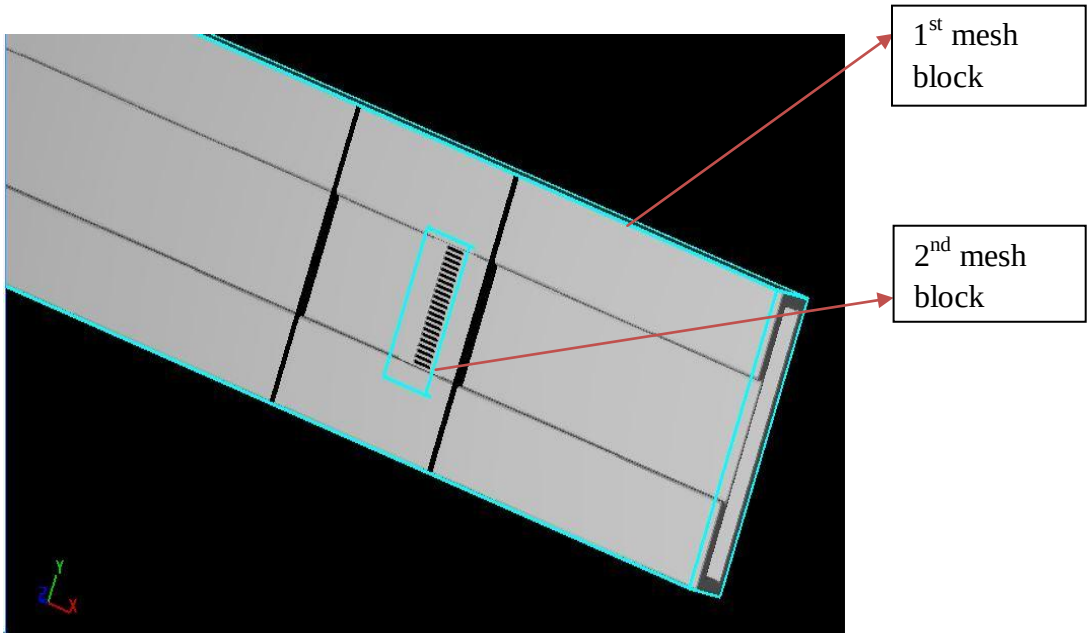

Figure 5.7 Final Geometry of Model

5.3.4 Baffle for Flow Rate Indicator

In the laboratory experience, water flow is given by a source and water was carried by channels. There are three channels under three continuous grates and three pools related to those channels and extra pool for the bypass flow. Water was collected in these pools and calculations were carried by under the aid of this system. System in the laboratory (Sipahi, 2006) is illustrated in Figure 5.8.

Figure 5.8a Eperimental Setup(Channels under Grates)

Figure 5.8bExperimental Setup (Pools for Water Collecting System)

While modeling the system the baffle option gave us opportunity to eliminate pool system and add baffle block instead. Installation baffle block with %100 porosity will calculate volumetric flow rate passing through the baffle block. For this reason, three baffle blocks were added to system (Figure 5.9);

1. First baffle was located before the grate to calculate total flow passing through the system.
2. Second baffle was located under the grate to calculate intercepted flow by grate.
3. Third baffle was located after grate to calculate bypass flow.

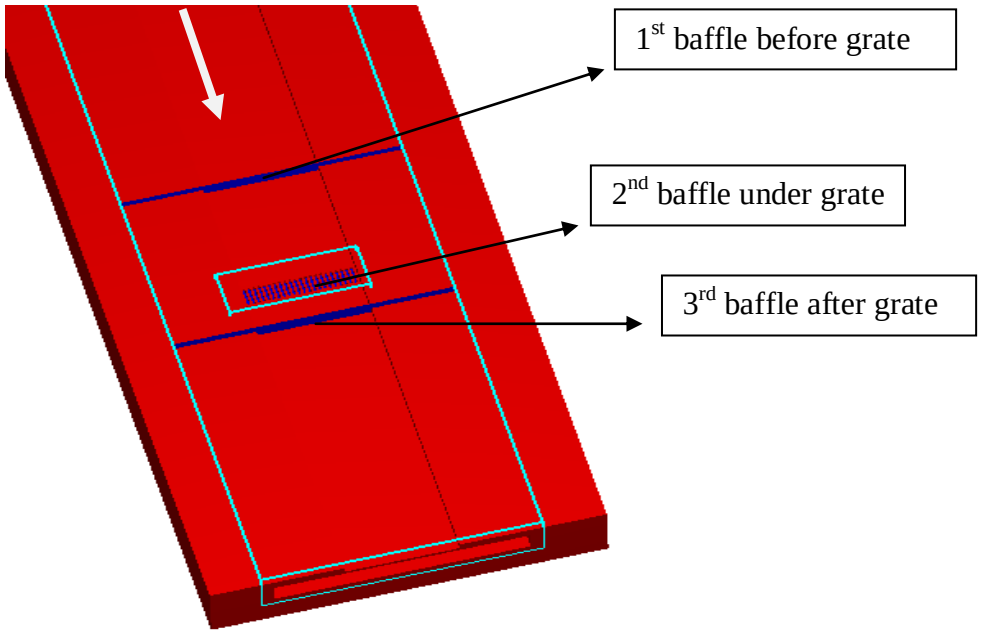

Figure 5.9 Baffle Blocks as Flow Rate Indicator

5.3.5 Boundary Conditions

Two blocks of meshes were considered as explained in previous headlines. Flow 3D software offers six boundary conditions for every mesh block. Hence, in this study 12 boundary conditions were assigned for two mesh blocks. 1st mesh block was very important for the accuracy of the calculations because boundaries of the model were assigned in that region and 2nd mesh block was defined only for detailed investigation of the grate result and to decrease number of the meshes.

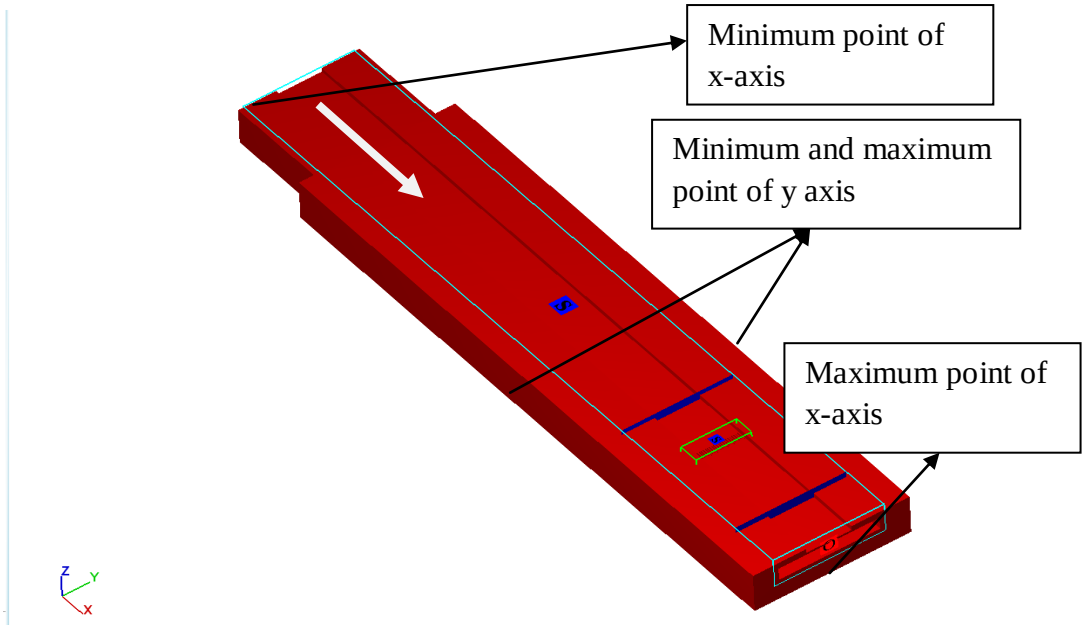

Figure 5.10 Boundary Conditions

As illustrated in Figure 5.10 different boundary conditions were assigned to the system. Boundaries were defined by using the minimum and maximum point of the axis. The orientation of coordinate system of the model was depicted at the left bottom of the Figure 5.12. Under this information, boundary condition at the min. point at x-axis is volumetric flow rate and flow depth. In the calculation stage different amount of discharges will be assigned at the minimum point of the axis. maximum point of the x-axis outflow boundary condition was assigned as illustrated in Figure 5.12. Since minimum and maximum point of y axis were represented the side walls of the model, walls boundary conditions were assigned. Finally, minimum point of z-axis was bottom of the model so wall type of boundary condition was assigned and at the top symmetry type of boundary conditions was used. For the second mesh block symmetry type of boundary condition were assigned for all of the boundaries since the grate system had carried same properties and geometry in every point.

5.3.6 Channel Capacity

It is important to calculate maximum depth of the flow for the model. The channel height of 0.1 m was taken as it was studied by Sipahi (2006). However, Sipahi (2006) used small amounts of discharge compare to this study so depths of the flows become more important. If the flow depth exceeds 0.1 m the model will be failed and it will not be valid for exceeding depth. For this reason flow depth was calculated by using Manning equation.

$$Q=A/n*R^{2/3}*S^{0.5} \quad (5.1)$$

Where Q is the total discharge (m^3/s), A is the wetted area of the channel, R is Hydraulic radius of the channel and S is the longitudinal slope of the channel, n is the Manning roughness coefficient.

If equation is rearranged for rectangular channel by using depth of flow as y and width of the channel as 0.9 m and n=0.01 Sipahi (2006) and S=0.01 following equation will be obtained;

$$Q=0.9y/0.01*(0.9y/(2y+0.9))^{2/3}*0.01^{0.5} \quad (5.2)$$

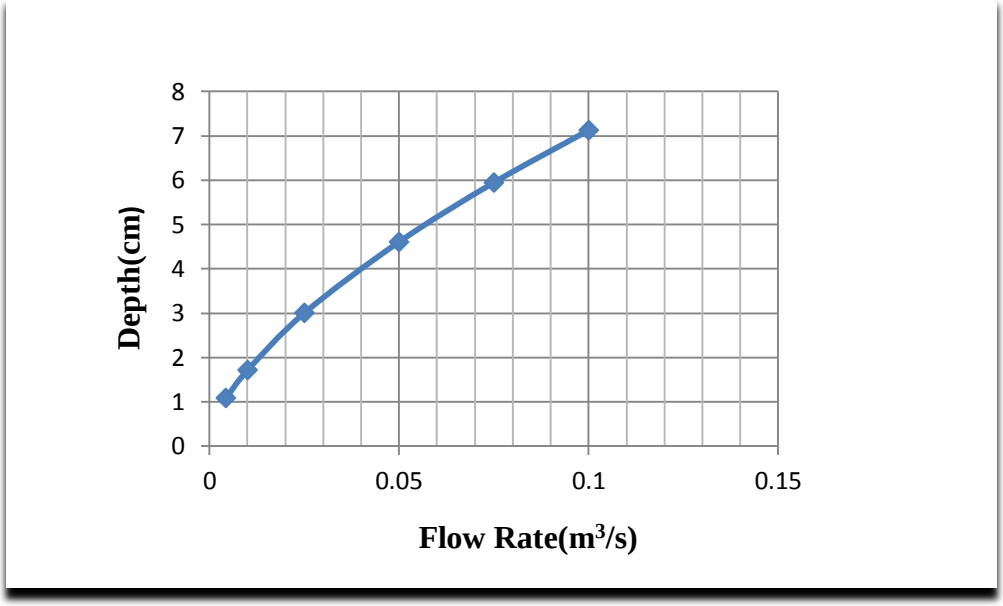

Figure 5.11 Flow Depths vs. Flow Rate Graph

As illustrated above figure flow depths were not exceeded maximum height of the channel, so studying on them will not cause any problem when thickness of the wall was considered.

5.3.7 Model Run

Model, built by Flow 3D, run for different flow rates and run times. Since, total flow given from the upstream have to be satisfied at the downstream, measurement of time is calculated by using the principal of the mass conservation. Firstly, the model was simulated in 10 seconds (computational time of 3 hours) and it was observed that the flow was reached steady state at the first baffle block before grate; however, total amount of flow rates tends to increase for the downstream of the grate. Since, amount of flow passing from the first grate should be accumulated from second and third baffle blocks, we decided to increase time of the simulation. The simulation of the model is depicted from Figure 5.12-5.13.

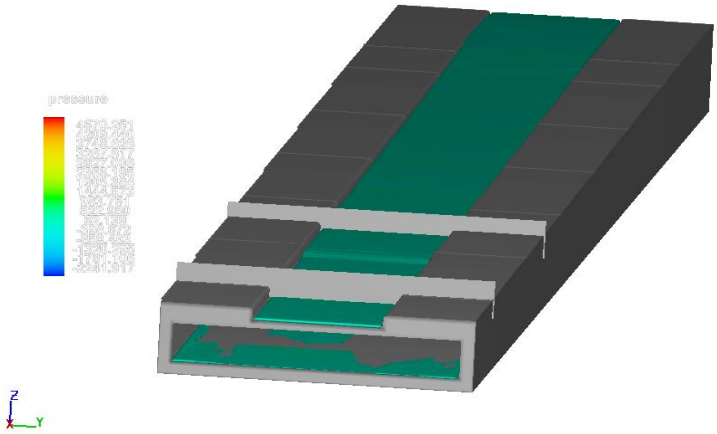

Figure 5.12 3D view of the simulation Q=0.1 m^3/sec t=10 sec.

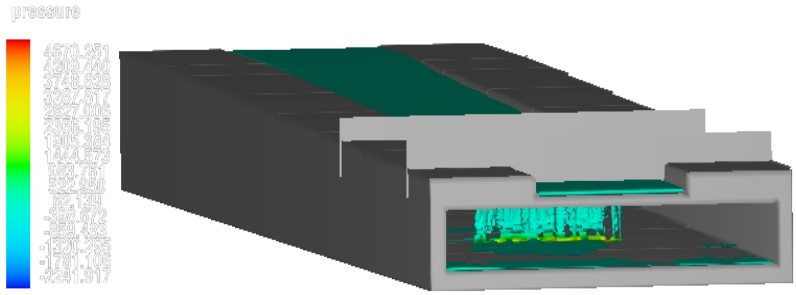

Figure 5.13 3D view of the simulation Q=0.1 m^3/sec t=10 sec.

After that, simulation time was increased to 30 seconds (computational time of approximately 20 hours) and observed that total amount flow passing from the first baffle was equal to total flow passing from the grate and by-pass flow over the grate. Furthermore, time of simulation was accepted as 30 seconds and implemented for all of the flows. In addition, flow versus time graph for three baffles which will be illustrated at chapter 6 will clearly show that 30 seconds simulation is sufficient for our measurement and generally, flow reaches its steady rates after 25 seconds. For different flow rates totally 16 simulation were rendered. Results of the simulations will be given in chapter 6.

CHAPTER 6

ANLAYSIS OF THE RESULTS AND DISCUSSION

After modeling the experimental model of Sipahi (2006) numerical calculations were carried out for nine different discharges and total flow, intercepted flow and by-pass flow rates were taken as output of the simulation.

Table 6.1 Flow Rates Obtained from Numerical Model

No	Total Flow Rate (m^3/s)	Intercepted Flow Rate (m^3/s)	By-Pass Flow Rate (m^3/s)
1	0.00427	0.0036	0.0002
2	0.0100	0.0100	0.0000
3	0.0250	0.0241	0.0006
4	0.04995	0.0422	0.0074
5	0.0750	0.0422	0.0234
6	0.1000	0.0488	0.4814
7	0.2000	0.0595	0.1375
8	0.3500	0.0766	0.2638
9	0.5000	0.0850	0.3760

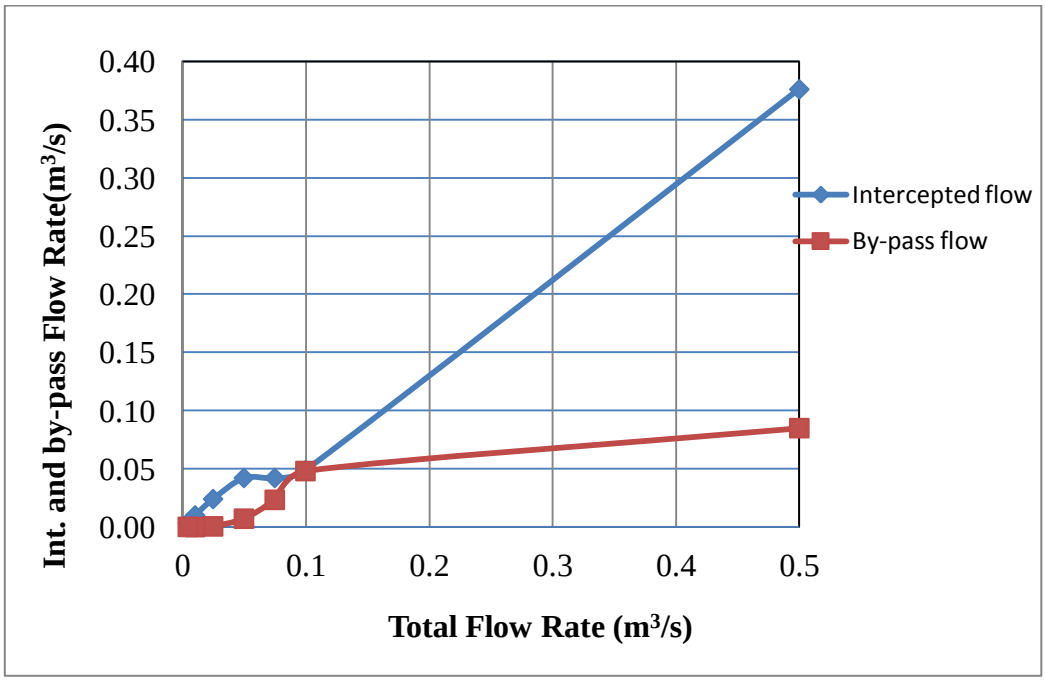

Figure 6.1 By-Pass and Intercepted Flow Rate versus Total Flow Rate Graph

Simulation process was taken as 30 seconds generally to reach upstream flow steady stage. Flow rate quantities which were being passed from the baffles were shown in the figures below. For each amount of discharges the same procedure was applied and all of the results were recorded. Values of the flow rates are presented in Table 6.1 and Figure 6. Figures 6.2 to 6.19 illustrates flow rates versus time graph.

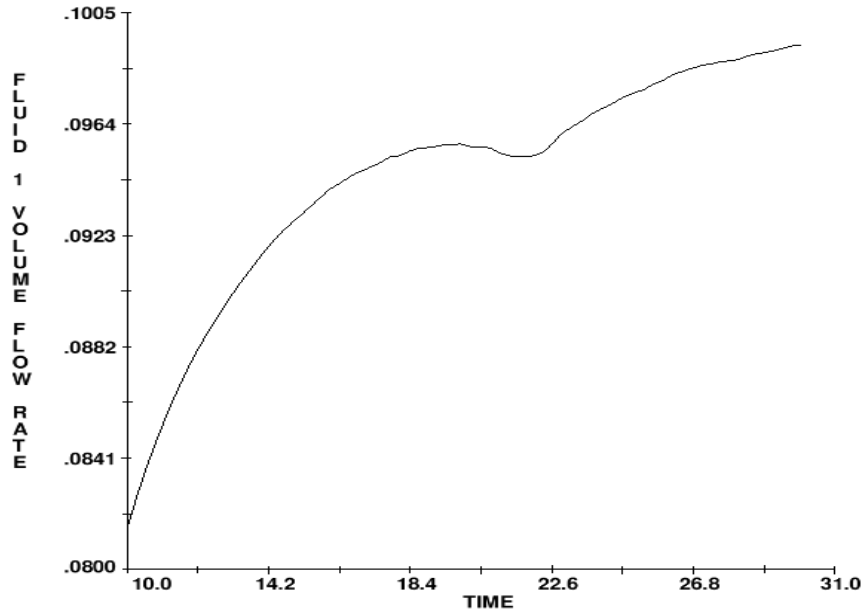

Figure 6.2 Flow Rate Graph for Q=0.100 m^3/s (Total Flow)

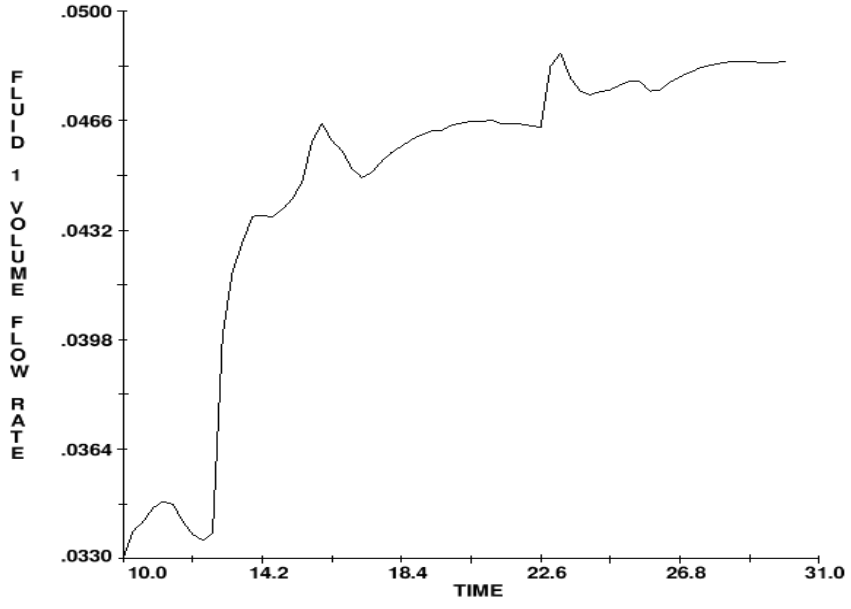

Figure 6.3 Flow Rate Graph for Q= 0.100 m^3/s (By-Pass Flow)

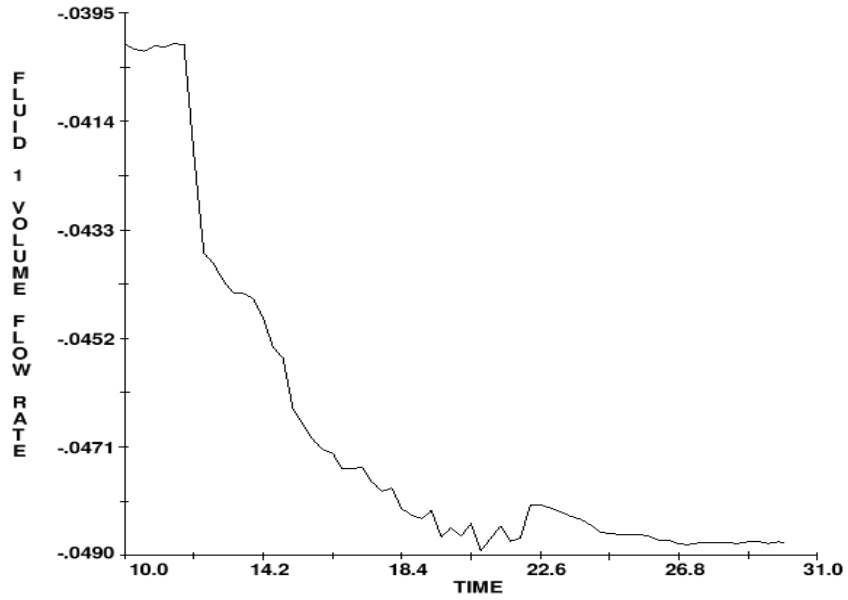

Figure 6.4 Flow Rate Graph for Q= 0.100 m^3/s (Intercepted Flow)

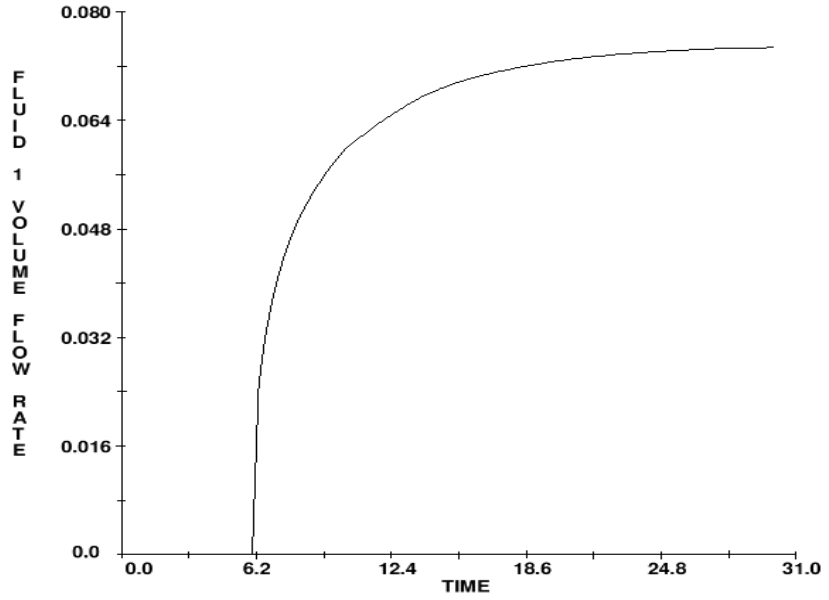

Figure 6.5 Flow Rate Graph for Q=0.075 m^3/s (Total Flow)

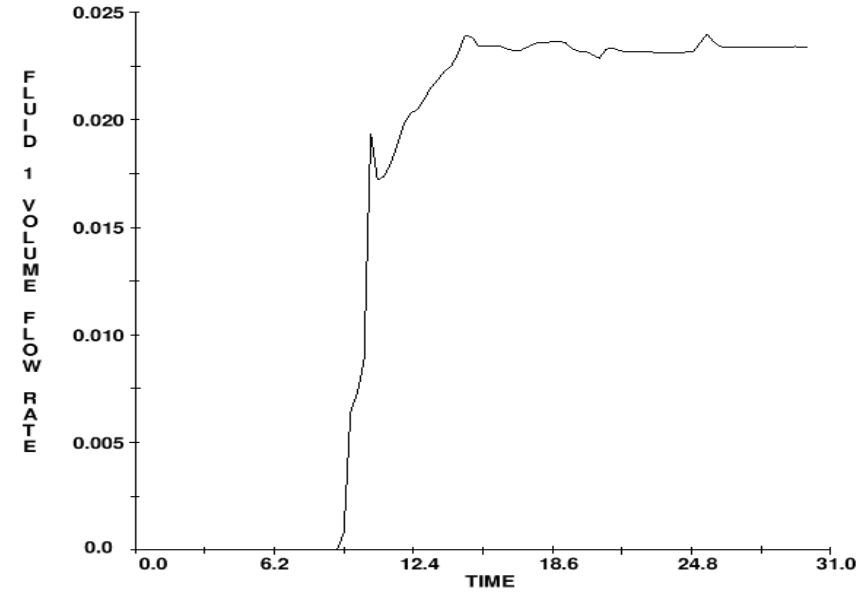

Figure 6.6 Flow Rate Graph for Q=0.075 m^3/s (By-Pass Flow)

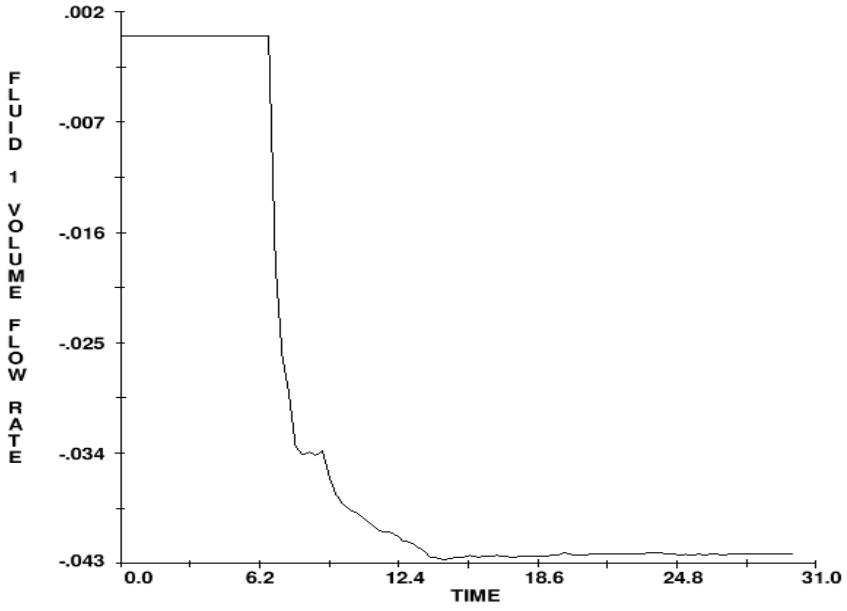

Figure 6.7 Flow Rate Graph for Q= 0.075 m^3/s (Intercepted Flow)

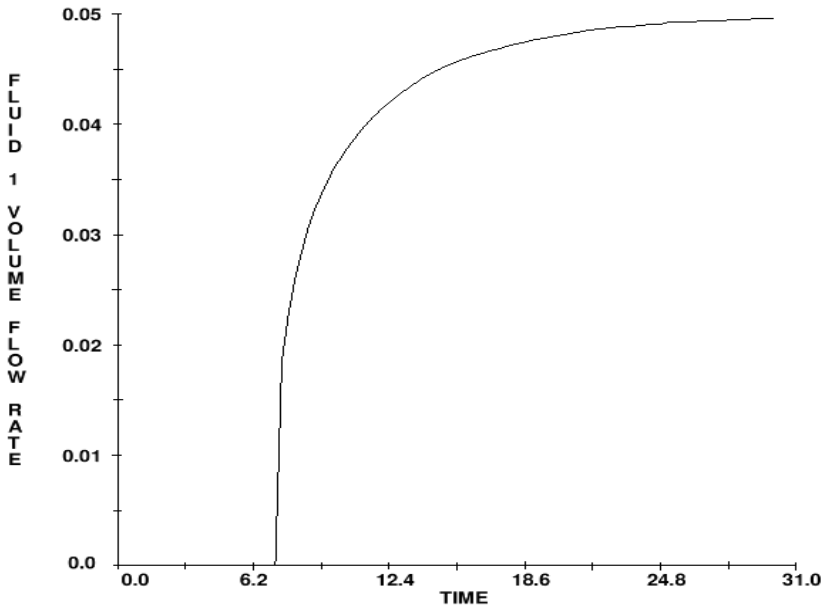

Figure 6.8 Flow Rate Graph for Q=0.04995 m^3/s (Total Flow)

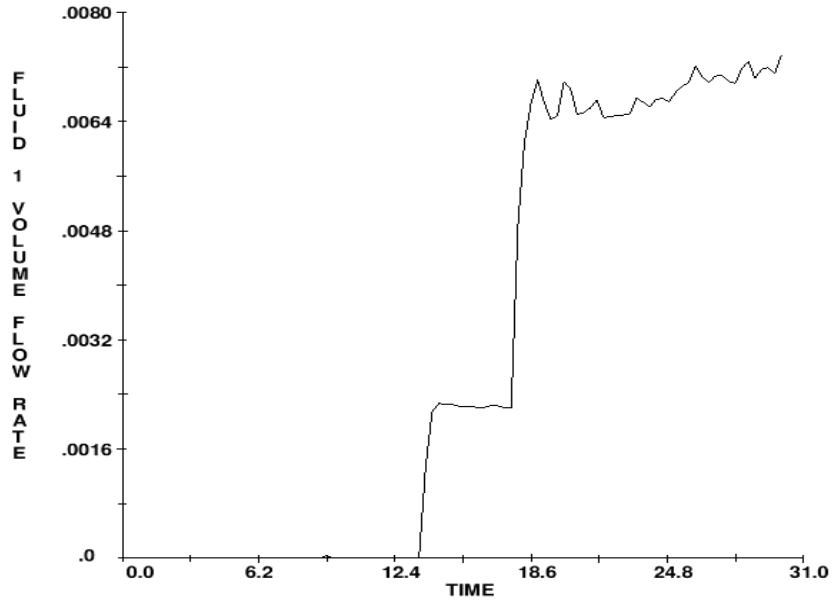

Figure 6.9 Flow Rate Graph for Q=0.04995 m^3/s (By-Pass Flow)

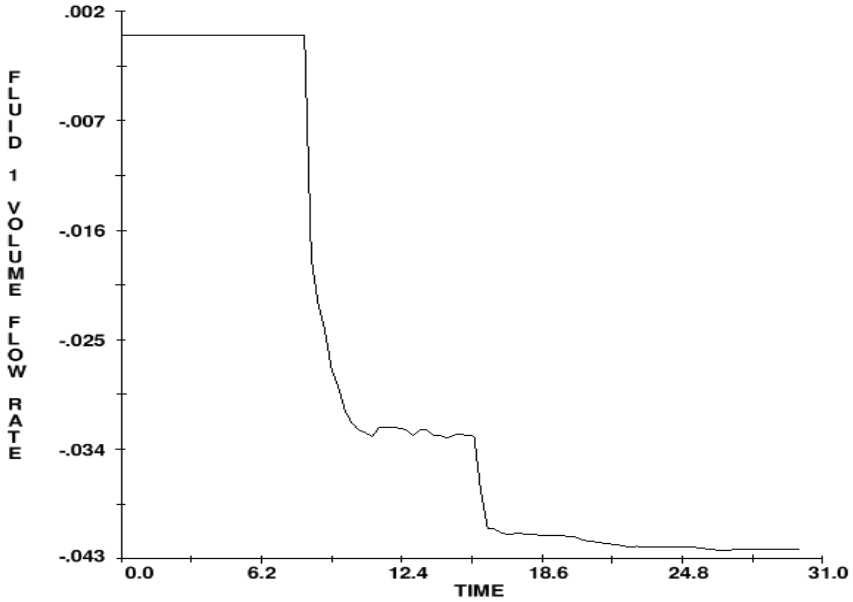

Figure 6.10 Flow Rate Graph for Q= 0.04995 m^3/s (Intercepted Flow)

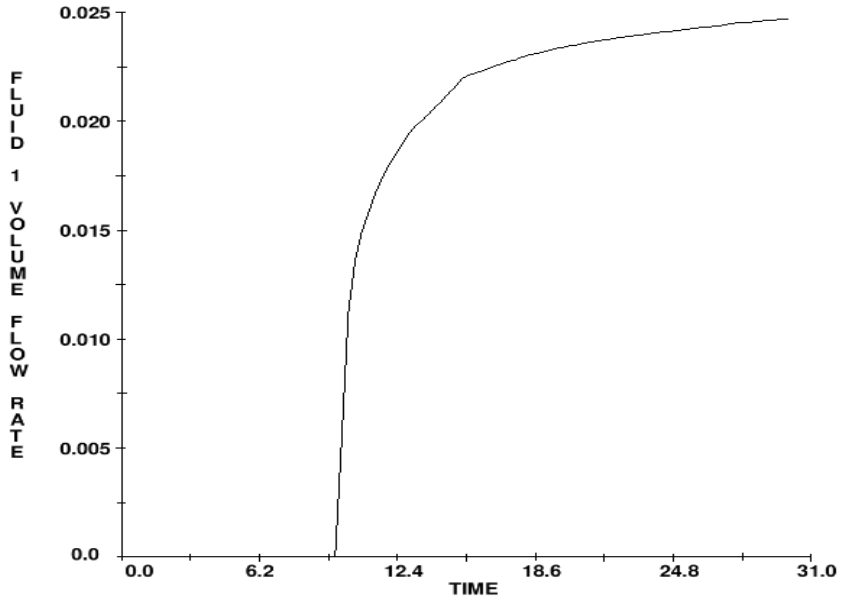

Figure 6.11 Flow Rate Graph for Q=0.025 m^3/s (Total Flow)

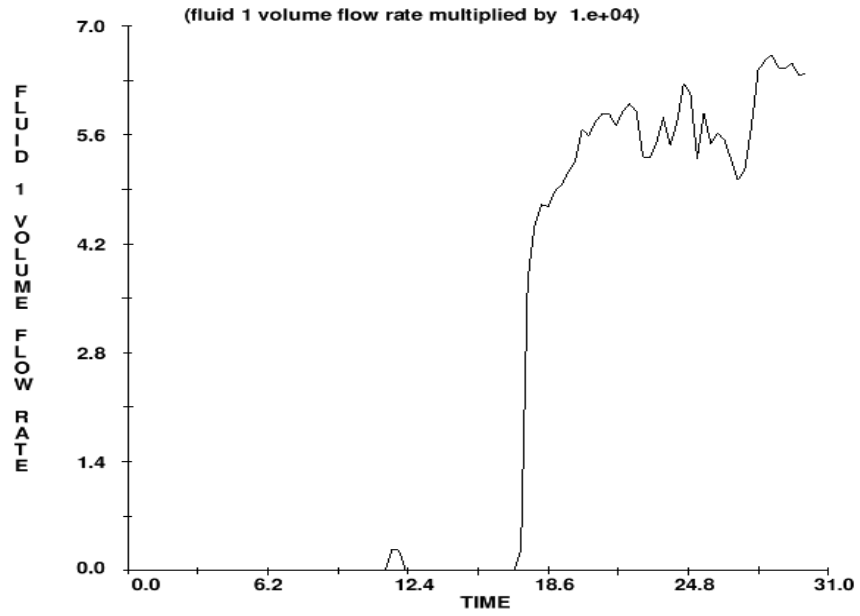

Figure 6.12 Flow Rate Graph for Q=0.025 m^3/s (By-Pass Flow)

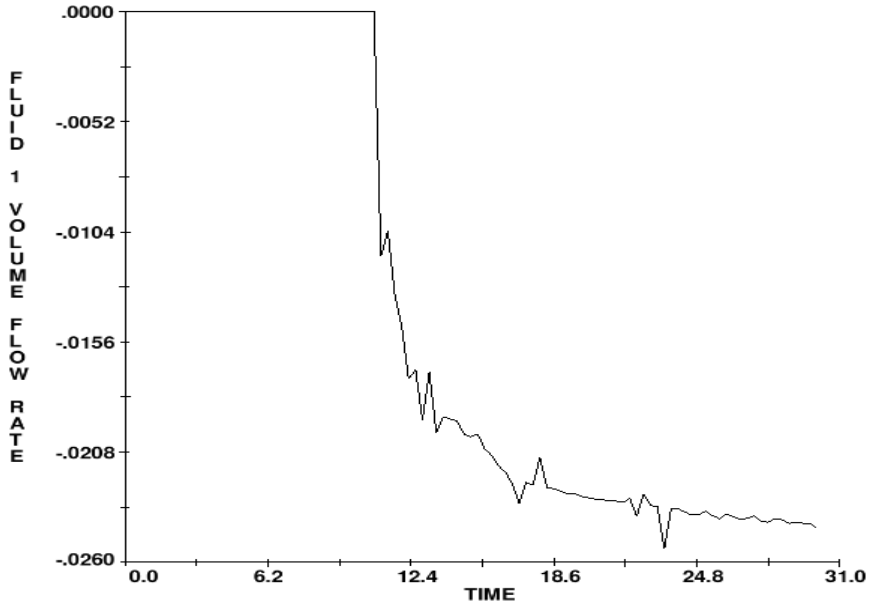

Figure 6.13 Flow Rate Graph for Q= 0.025 m^3/s (Intercepted Flow)

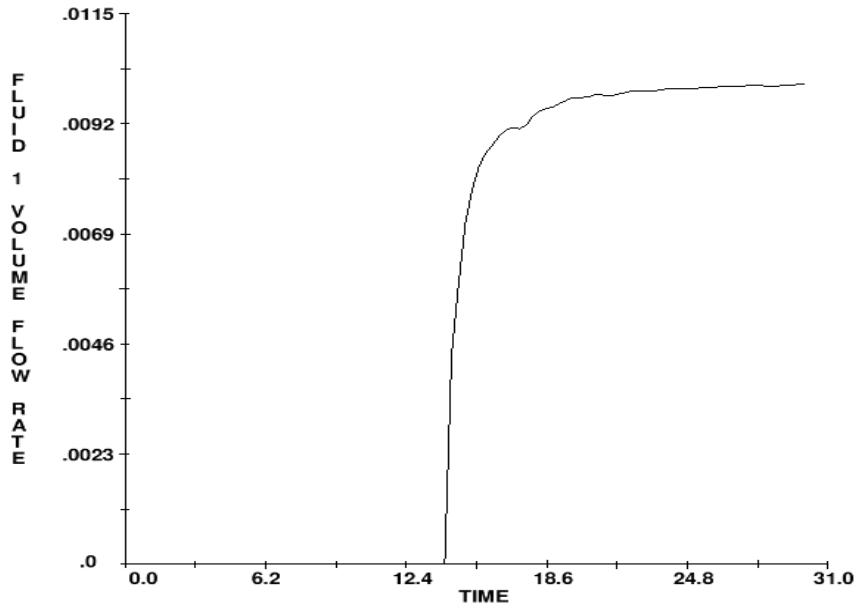

Figure 6.14 Flow Rate Graph for Q=0.01 m^3/s (Total Flow)

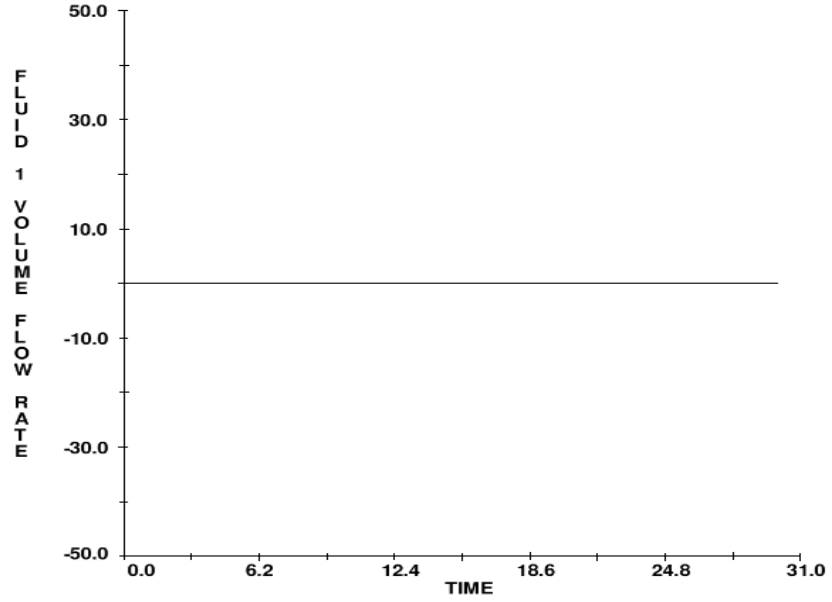

Figure 6.15 Flow Rate Graph for Q=0.01 m^3/s (By-Pass Flow)

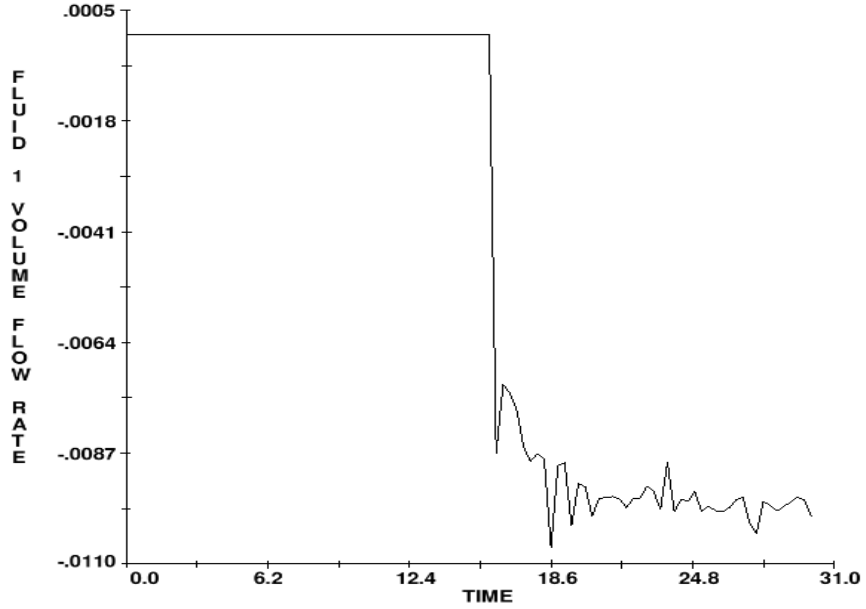

Figure 6.16 Flow Rate Graph for Q=0.01 m^3/s (Intercepted Flow)

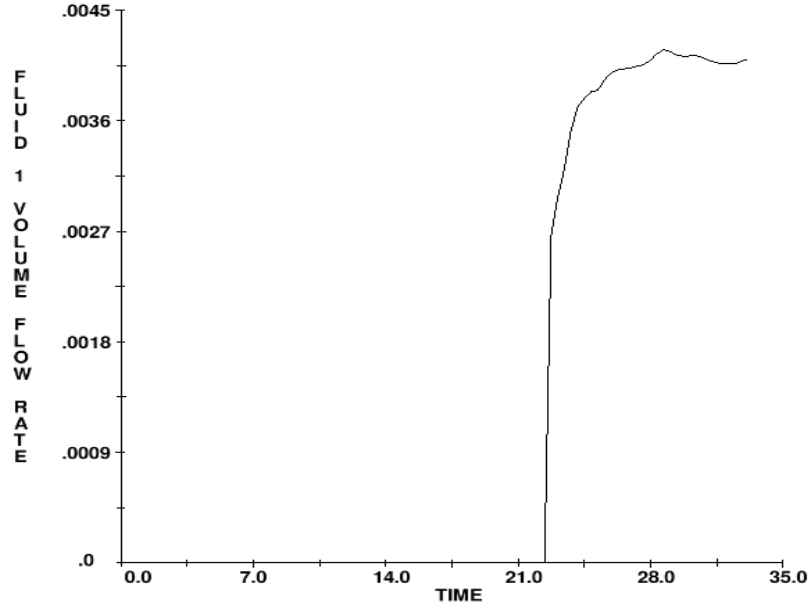

Figure 6.17 Flow Rate Graph for Q=0.00427 m^3/s (Total Flow)

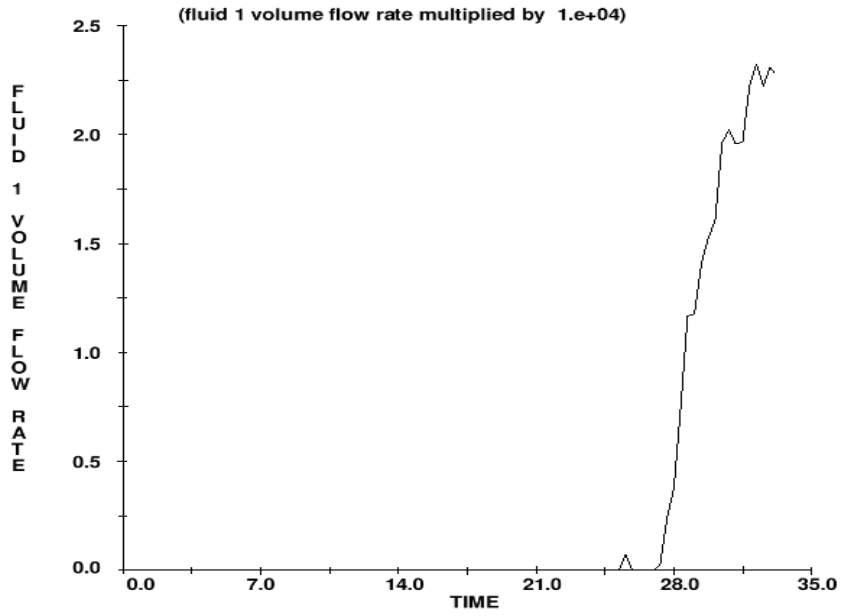

Figure 6.18 Flow Rate Graph for Q=0.00427 m^3/s (By-Pass Flow)

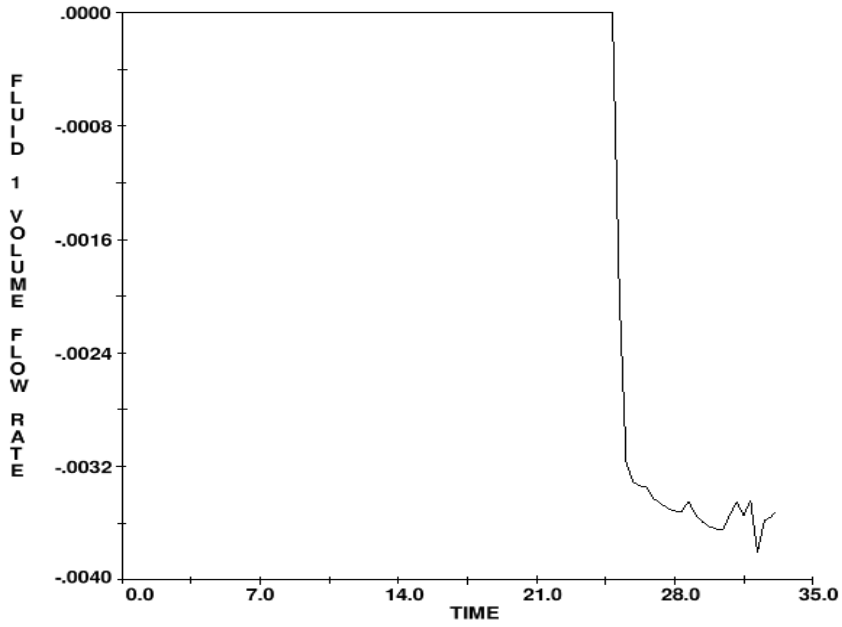

Figure 6.19 Flow Rate Graph for Q=0.00427 m^3/s (Intercepted Flow)

Flow rates until 0.1 m^3/s were investigated with the model of having 10 cm side wall. Another simulation was created to see behavior of grates for higher flow rates. As it is mentioned before, the height of the side walls were extended to 28 cm to increase the channel capacity and all the other properties remained as they were in the original one(Figure 6.20). Finally, flow rates of 0.20, 0.35, 0.50 m^3/sec were applied to system and results of the simulation were given in the Figures 6.21-6.29.

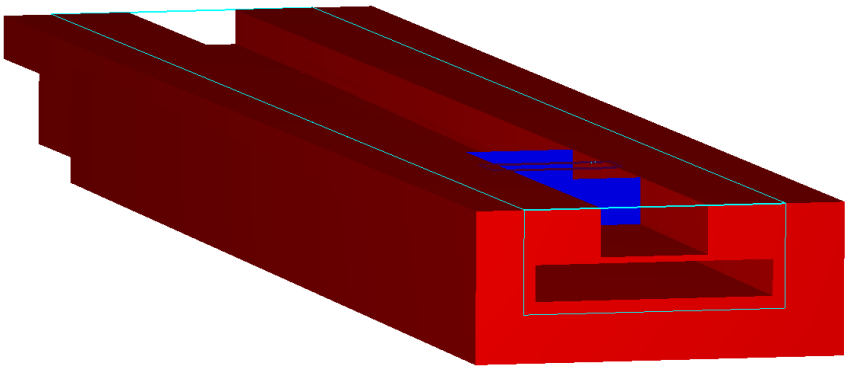

Figure 6.20 3D View of the Model for 0.50 m^3/sec

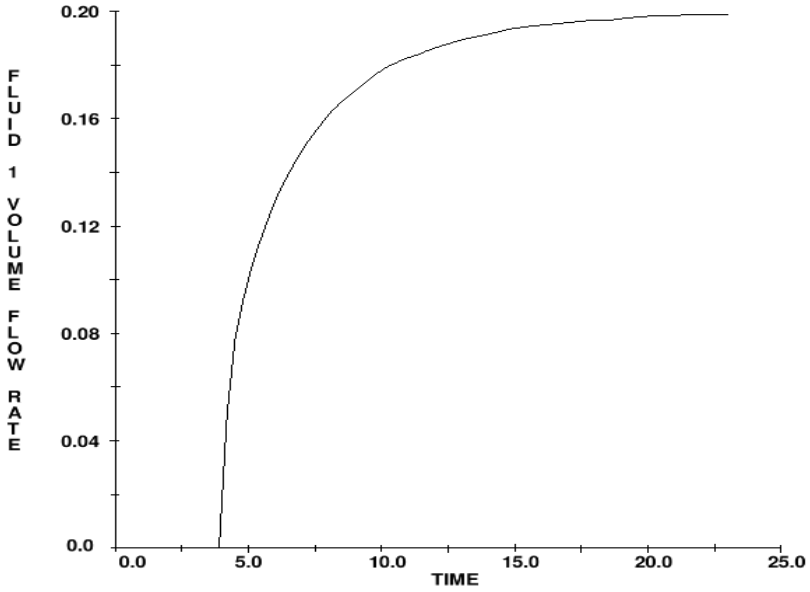

Figure 6.21 Flow Rate Graph for Q=0.20 m^3/s (Total Flow)

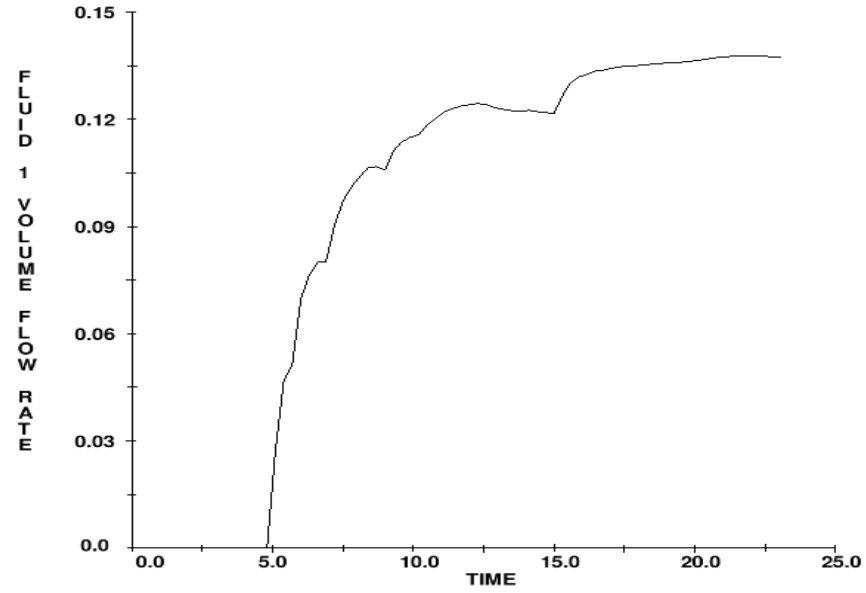

Figure 6.22 Flow Rate Graph for Q=0.20 m^3/s (By-Pass Flow)

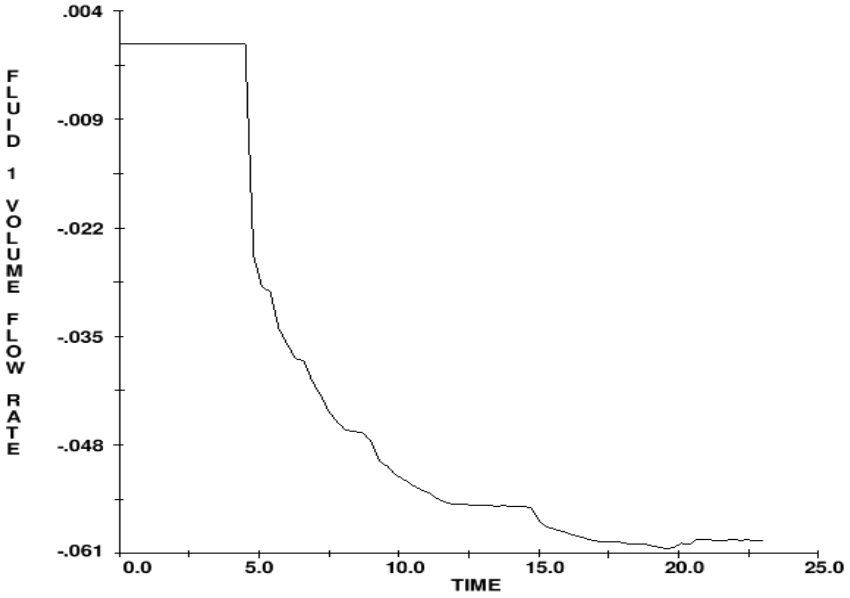

Figure 6.23 Flow Rate Graph for Q=0.20 m^3/s (Intercepted Flow)

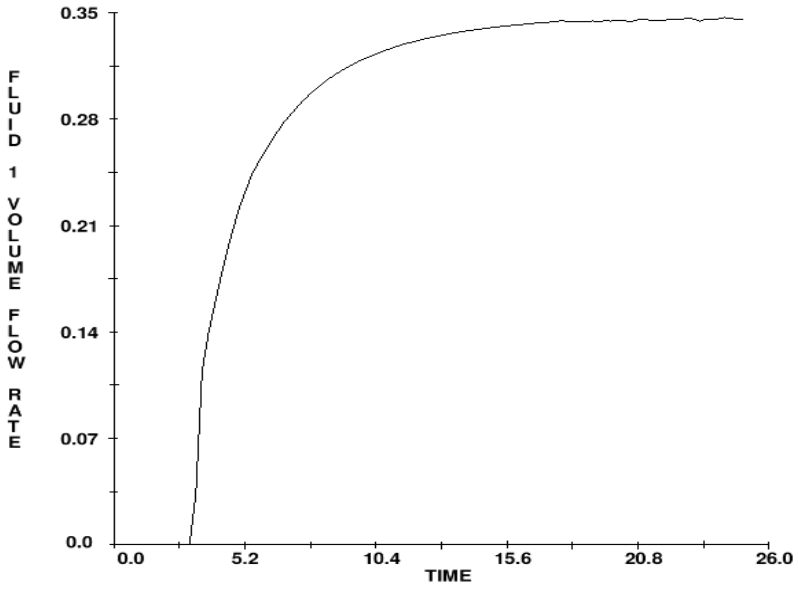

Figure 6.24 Flow Rate Graph for Q=0.35 m^3/s (Total Flow)

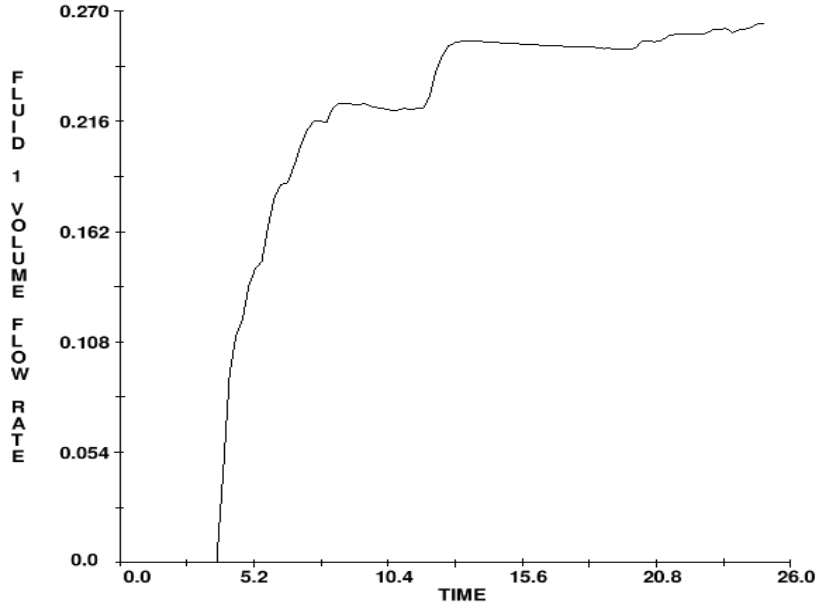

Figure 6.25 Flow Rate Graph for Q=0.35 m^3/s (By-Pass Flow)

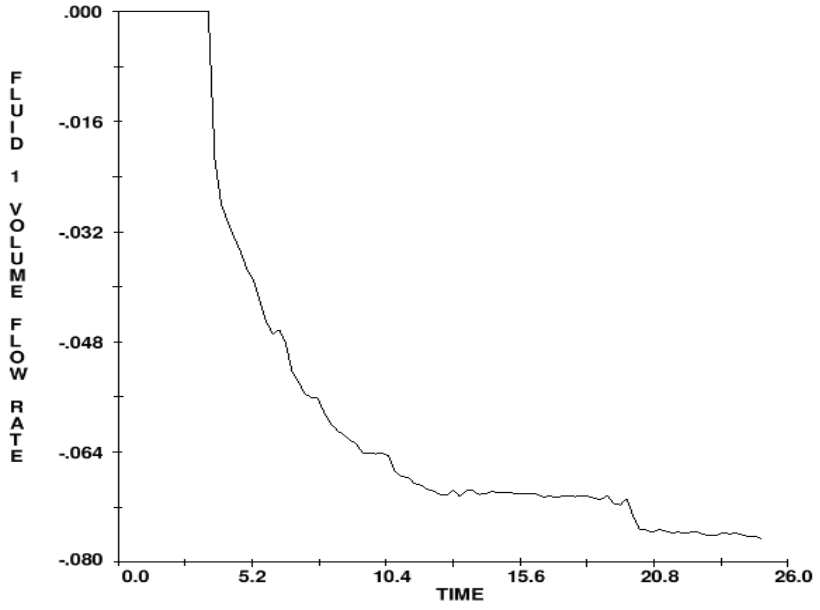

Figure 6.26 Flow Rate Graph for Q=0.35 m^3/s (Intercepted Flow)

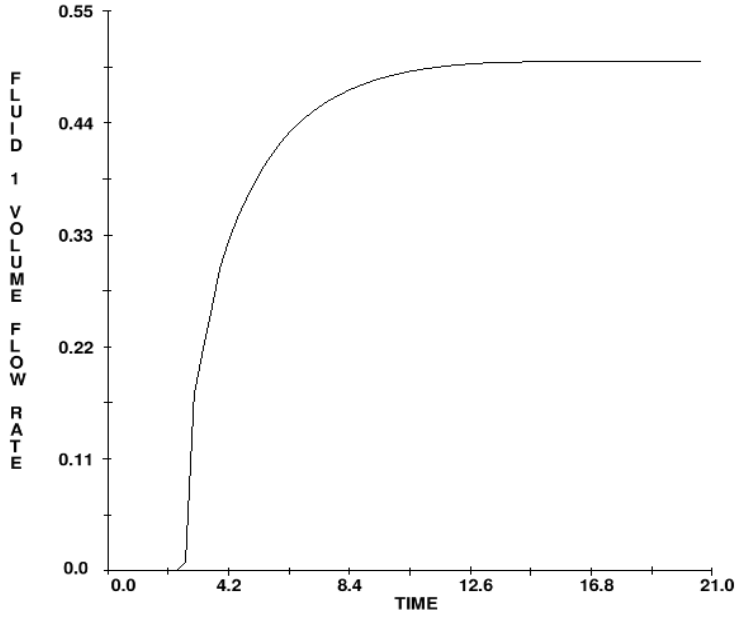

Figure 6.27 Flow Rate Graph for Q=0.50 m^3/s (Total Flow)

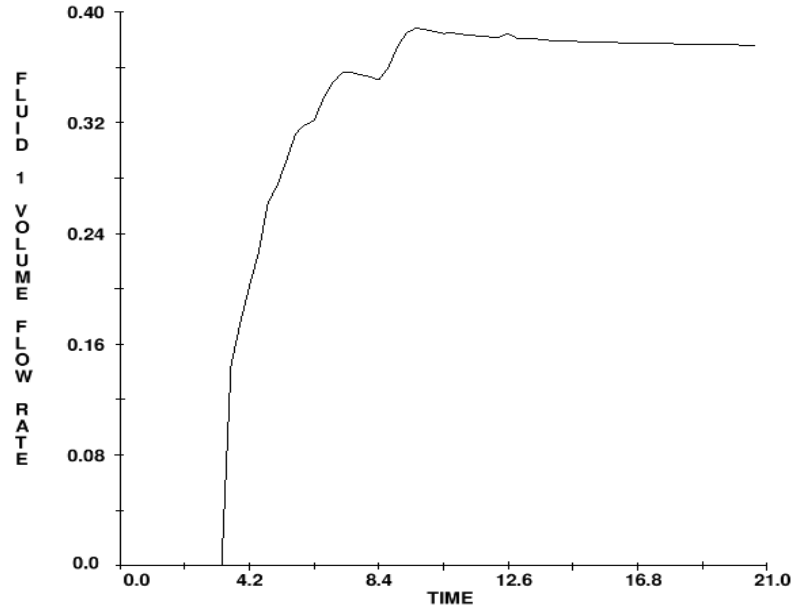

Figure 6.28 Flow Rate Graph for Q=0.50 m^3/s (By-Pass Flow)

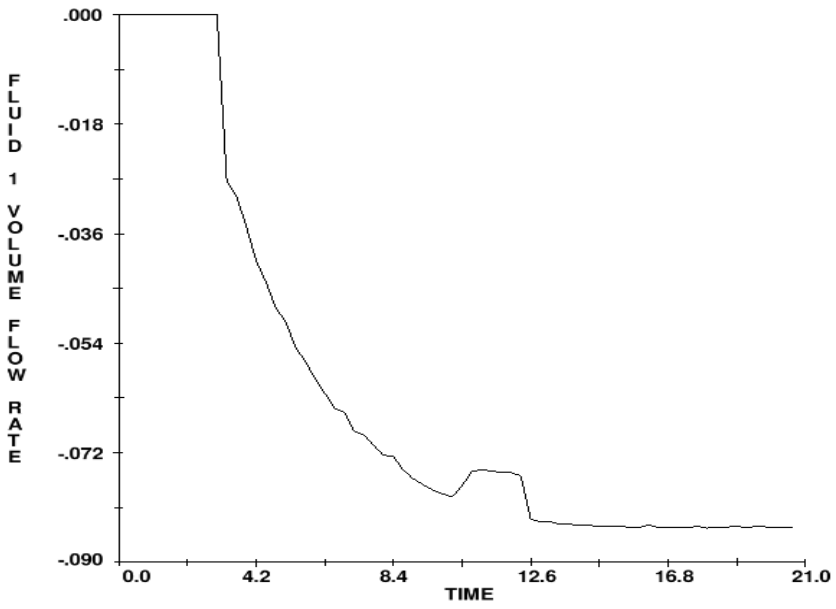

Figure 6.29 Flow Rate Graph for Q=0.50 m^3/s (Intercepted Flow)

6.1 Discharge and Efficiency

In order to see future manner of the flow additional simulation with Q_T=0.20, 0.35, 0.50 m^3/sec were performed. Since, water depth related to flow rates is higher than our side walls height, which is 10 cm, side walls of the channel is extended to 28 cm and analyzed were performed. Finally, total flow versus efficiency graph was obtained and results of the model are illustrated on Figure 6.30.

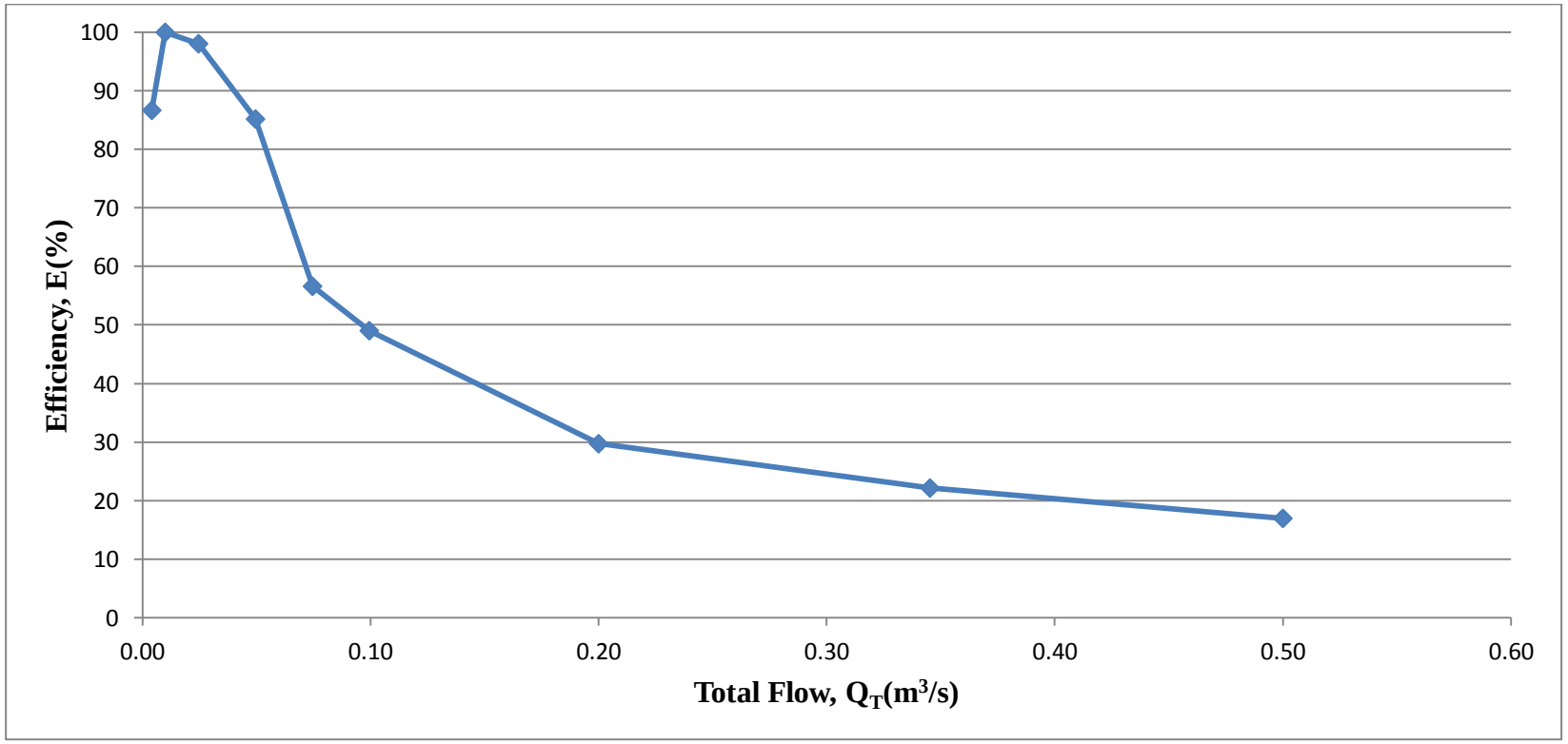

Figure 6.30 Total Flow vs. Efficiency Graph. From Computer Model

As seen in the Figure 6.30 the efficiency versus total flow graph is very similar to bell shaped curve. It is observed that efficiency of grate is increasing with the increased total flow until it reaches the peak value and after that it is started to decrease. It is expected that efficiency will decrease as flow rate and depths increase (HEC 22, 1991), (McEnroe,et al, 1999). As the flow rate increase velocity and water depths are also increased and with the higher velocity fluid particle can splash over the grate easily. When velocities of the flow rates are lower, fluid particles are passing over the grates with lower velocity so that efficiencies are increasing at the first leg of the curve. When, flow rates and velocities are increased, amount of fluid particle that pass over the grates are also increased so the efficiencies of grate are decreased at the second leg of the curve as it is expected. Velocity profiles of the fluid particles are taken from the model as seen in Figure 6.31. The velocity profiles were taken at 1 meter before grate and in the centerline of the channel cross section. For velocities of other flow rates please refer Appendix A.

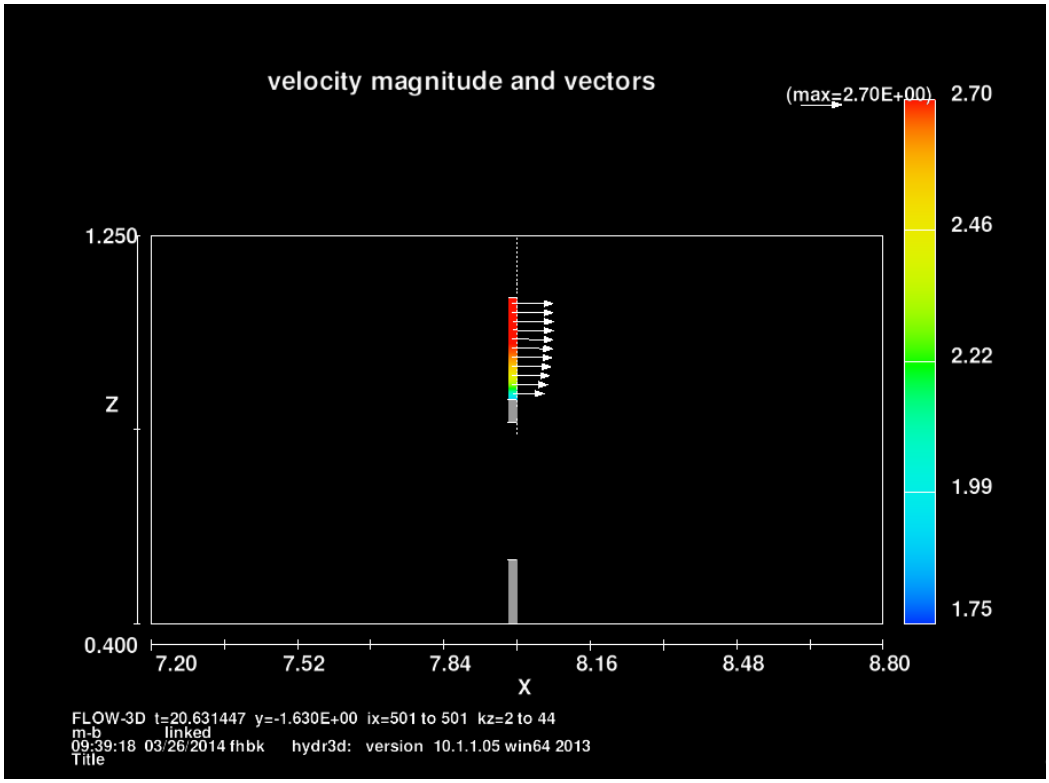

Figure 6.31 Velocity profile of Fluid Particles before Grates for Q_T=0.5 m^3/s

If, efficiency results of the numerical model, Sipahi (2006) and Gomez and Russo (2009) are combined on the same graphic Figure 6.32 is obtained.

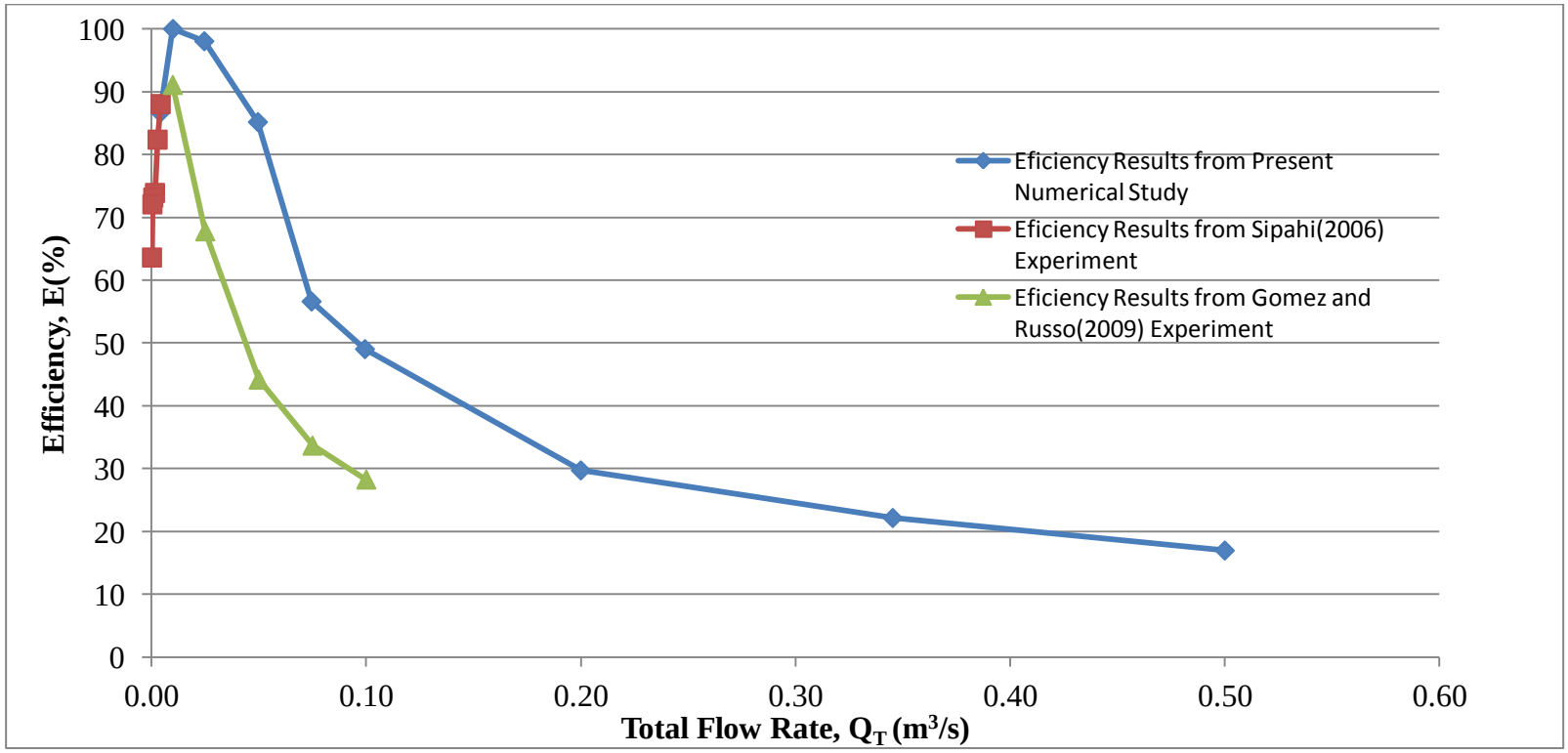

Figure 6.32 Total Flow Rate vs. Efficiency Curve Combined with Results of Sipahi (2006) , Gomez and Russo (2009) and Numerical Model of Present Study

As it is illustrated in the Figure 6.32 the results of Sipahi (2006) and numerical model are intercepted each other. Furthermore, it can be emphasized that results of the numerical model are accurate. However, Gomez and Russo (2009) results are located under that curve. It was an expected result, since grate of Gomez and Russo (2009) not fully covered the platform, in other words, platform width is 1.5 m and grate width is 1.0 m so, there are 0.25 m gaps between side walls and grates so that water can passed through that gaps. For this reason, bypass flow increased and intercepted flow and efficiencies are decreased.

6.2 Froude Number in Efficiency

Since water depth and velocity of the flow varies through the channel, the Froude numbers at steady state conditions are investigated. Flow depths were calculated by using Manning's equation, and average velocities of the flow determined with related discharges. Since the cross section of the channel is constant through flow and the channel is rectangular Froude number is directly related with total flow Q_t and related depth. Froude numbers of the related discharges are obtained by using equation 6.1.

$$Fr=V_{avg}/(g*y_n)^{0.5} \quad (6.1)$$

Where;

V_{avg} is average velocity, g is acceleration of gravity and y_n is uniform water depth.

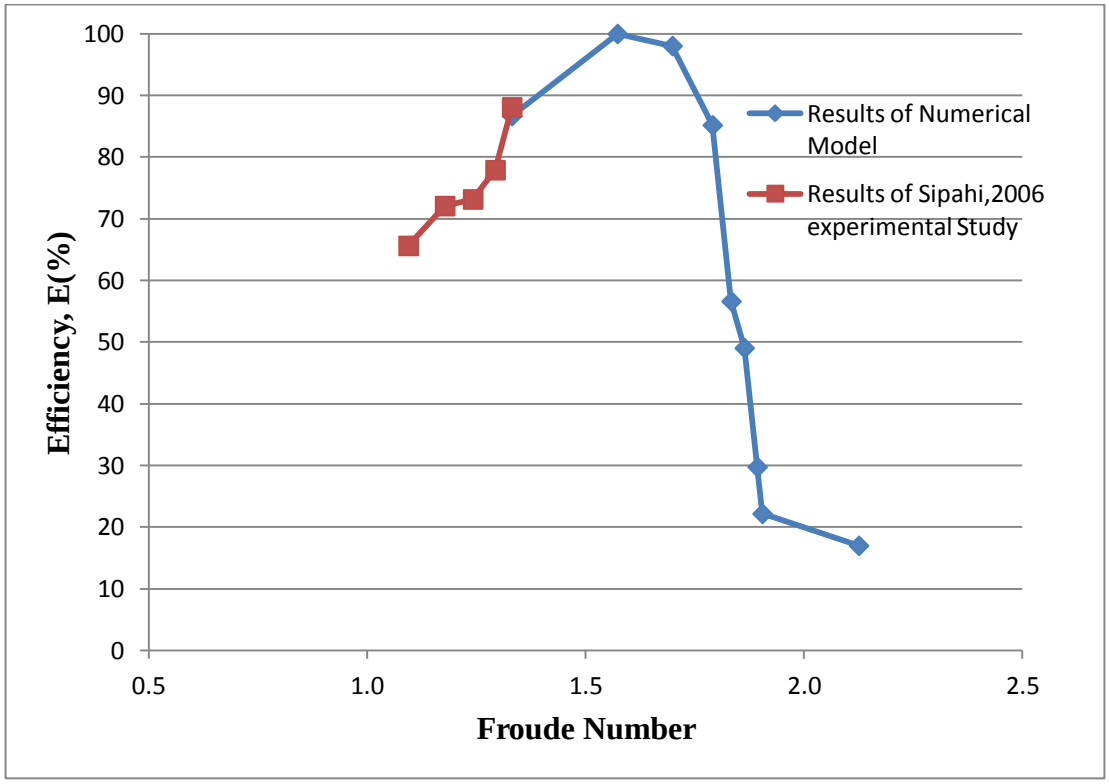

Figure 6.33 Froude Number vs. Efficiency Curve at Steady State Conditions

As it was expected, the results have same behavior as Efficiency versus Total Flow Rate graphic. In this respect, efficiency of the channel can also be represented by Froude number (Tiğrek, Sipahi, 2011)

.

CHAPTER 7

CONCLUSION

In this study efficiency of grates are investigated by using Flow 3D software. A numerical approach is conducted to calculate intercepted flow by using single longitudinal slope of 1%. The computer model was created by using experimental studies. After examining the result, the following findigs can be expressed:

1. Efficiency rates with total flow has bell shaped curve. Hence, results should be investigated in two parts. The results and the recent experiments showed that with increasing flow rates efficiency of grate has tendency to increase until it reaches the peak point which is %100 and it starts to decrease.

2. Efficiency of grate and intercepted flow rate are influenced by longitudinal slope, total discharge and shape and width of the channel. If all of those parameters will be investigated in details empirical model can be proposed.

3. For higher flow rates, it can be emphasized that efficiencies are extremely decrease and called inefficient. This statement is also valid for very small flow rates.

4. Void ratio, numbers of grate bars and orientation of the bar are also deterministic data that could affect the result of the system. Hence, those parameters should be investigated in the future studies.

5. If the system needs to be adopted for highway design traverse slope should also be considered in the future studies.

REFERENCES

American Association of State Highway and Transportation Officials, Highway Drainage Guidelines "Vol. IV: Hydraulic Design of Highway Culverts." AASHTO, Inc., Washington, D.C, 1992.

A.S.C.E, Design Manual for Storm Drainage, Newyork, 1960.

Brown, S. A., S. M. Stein and J. C Warner. 1996. Urban Drainage Design Manual. Hydraulic Engineering Circular No. 22. FHWA-SA-96-278. Washington, D.C. U.S. Department of Transportation, Federal Highway Administration.

Chow, Ven Te. "Open-Channel Hydraulics", Mc-Graw-Hill, New York, 1959.

Flow 3D Lecture Notes, Hydraulic Training Class, 2012.

Flow 3D, v10.1 User Manuel, 2012.

Flow 3D, Advanced Hydraulics Training, 2012.

Gomez M, Russo B (2005) Comparative study among different methodologies to determine storm sewer inlet efficiency from test data. In: 10th international conference on urban drainage,Copenhagen/Denmark, 21–26 August 2005

Gomez M, Russo B (2009) Hydraulic efficiency of continuous transverse grates for paved areas. J Irrigation Drain ASCE 135(2):225–230

Gomez M, Russo B (2011) Methodology to estimate hydraulic efficiency of drain inlets. Water Manag, ICE, pp 1–10

Harlan Bengtson, Excel Spreadsheets for Design of Storm Water Drains and Their Inlets, 2010

Horton, R.E., 1933: The Role of Infiltration in the Hydrological Cycle, Trans. Am. Geophys. Union, Vol.14, pp.446-460.

Horton RE. 1945a. Erosional development of streams and their drainage basins: hydrophysical to quantitative morphology. Bulletin of the Geological Society of America 56: 275-370.

Kranc S.C., Anderson M.W. 1993. Investigation of Discharge through Grated Inlets. Final Technical Report, Florida Department of Transportation.

Manning, R., 1891: On the Flow of Water in Open Channel and Pipes, Trans. Inst. Civil Engrs., Ireland, Vol. 20, pp. 161-207, Dublin, Ireland.

Mc Enroe Bruce M., Wade Reuben P. and Smith Andrew K., HYDRAULIC PERFORMANCE OF CURB AND GUTTER INLETS, K-TRAN: KU-99-1 Final Report, 1999.

Mc Ghee, T.J., 1991.Water Supply and Sewerage, Singapore: Mc Graw Hill.

Mostkow M.A., Sur le calcul des grilles de prise d'eau (Theoretical study of bottom type water intake), La Houille blanche, Grenoble, 12th yr., no, pp. 570-580, September,1957.

Mostkow M.A., "Handbuch der Hydraulic" ("Open-Channel Hydraulics"), VEB Verkag Technic, Berlin, 1956,pp. 204-208 and 213-221.

Sipahi S.Ö, Calibration of a Grate on A Sloping Channel. M.Sc., Department of Civil Engineering, 2006.

Tiğrek Ş., Sipahi Ö., Rehabilitation of Storm Water Collection Systems of Urban Environment Using the Small Roads as Conveyance Channels, 2011.

U.S. Army Corps. of Engineers, HEC-22, Urban Drainage Design Manual, Hydrologic Engineering Center, Davis, California,1991.

APPENDICES

Appendix A. Velocity profile of the fluid particles

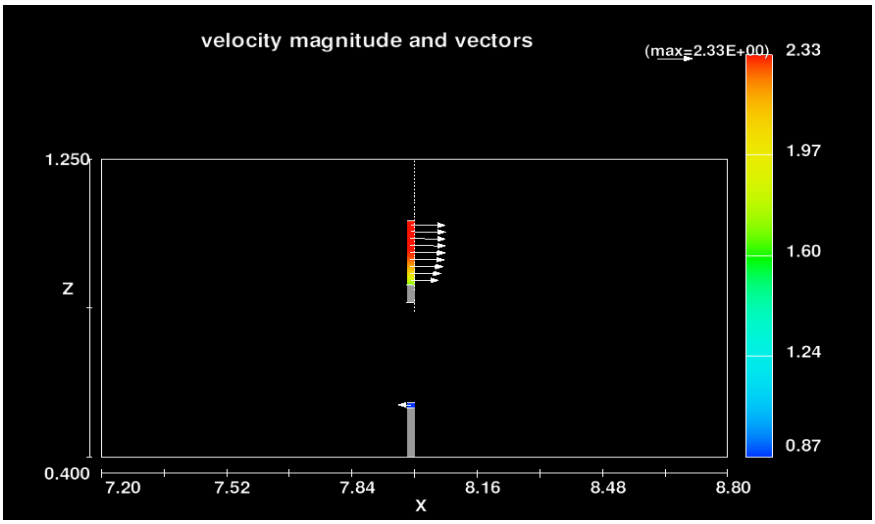

Figure A.1 Velocity profile of Fluid Particles before Grates for Q_T=0.35 m^3/sec

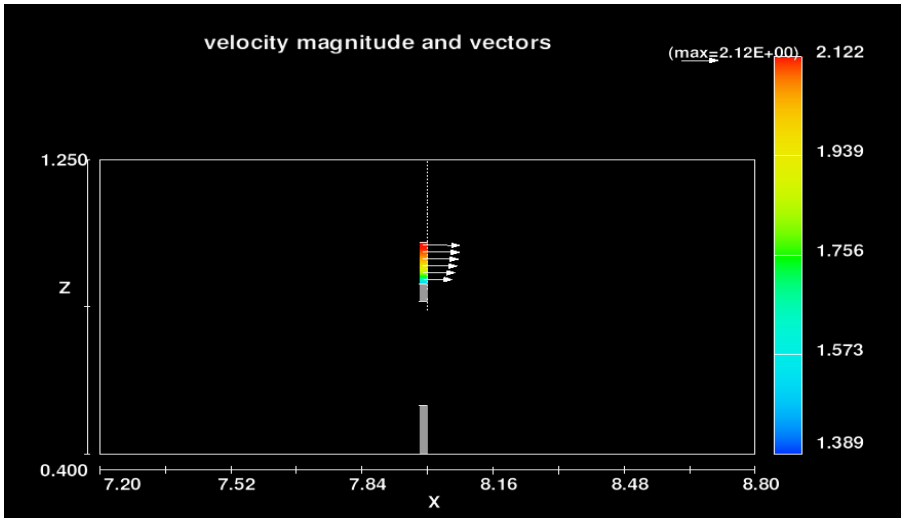

Figure A.2 Velocity profile of Fluid Particles before Grates for Q_T=0.20 m^3/sec

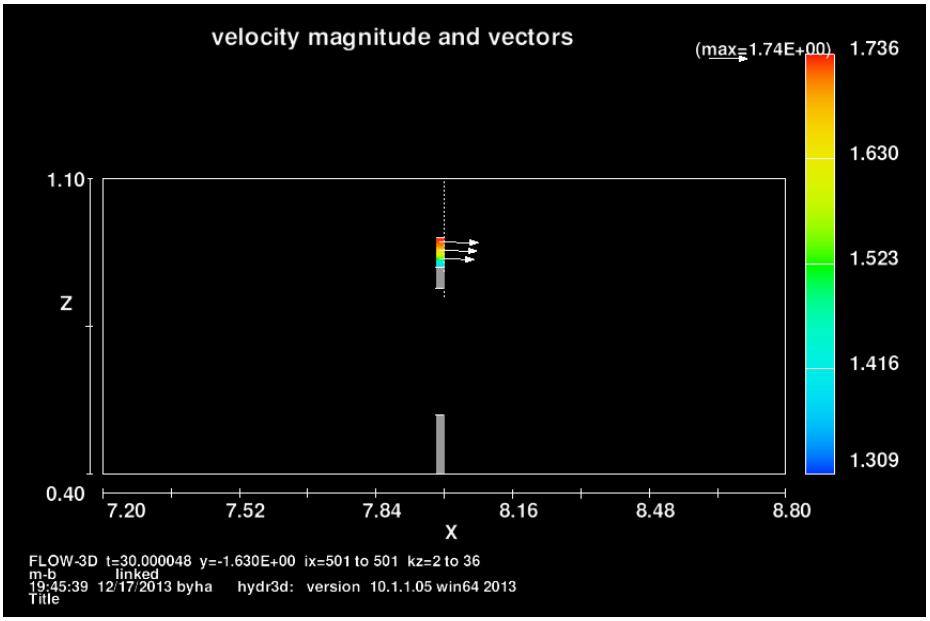

Figure A.3 Velocity profile of Fluid Particles before Grates for Q_T=0.1 m^3/sec

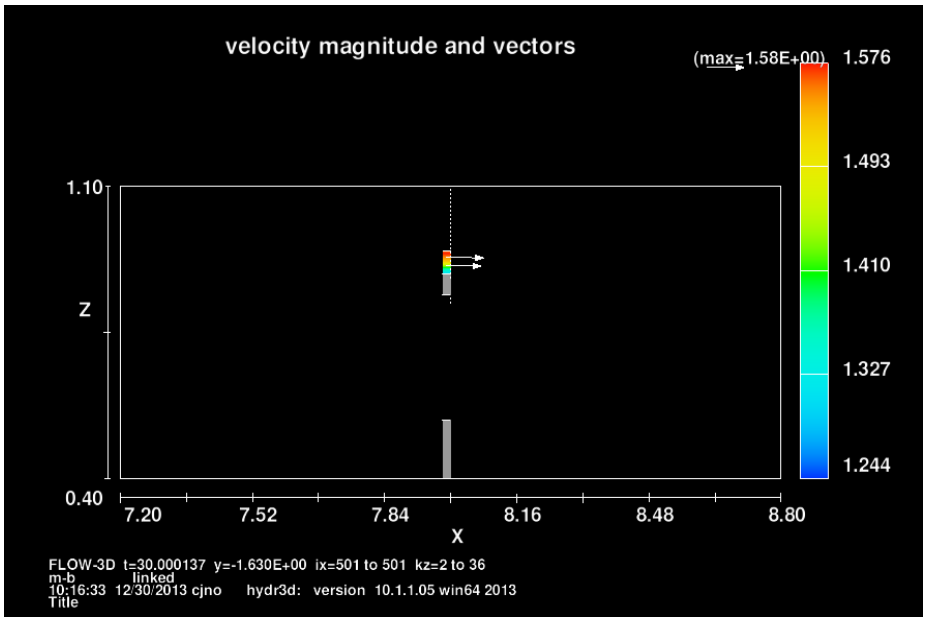

Figure A.4 Velocity profile of Fluid Particles before Grates for Q_T=0.075 m^3/sec

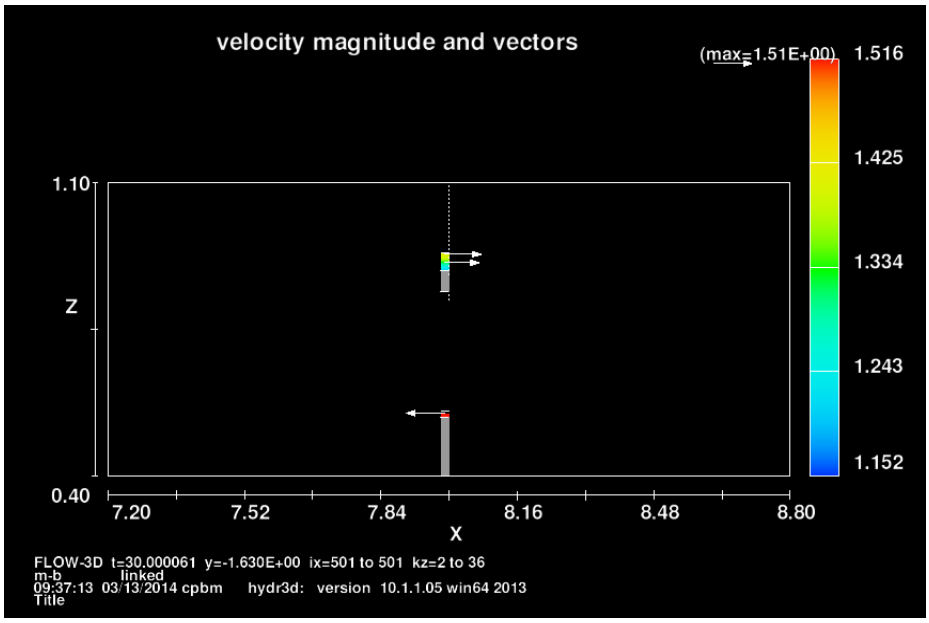

Figure A.5 Velocity profile of Fluid Particles before Grates for Q_T=0.04995 m^3/sec

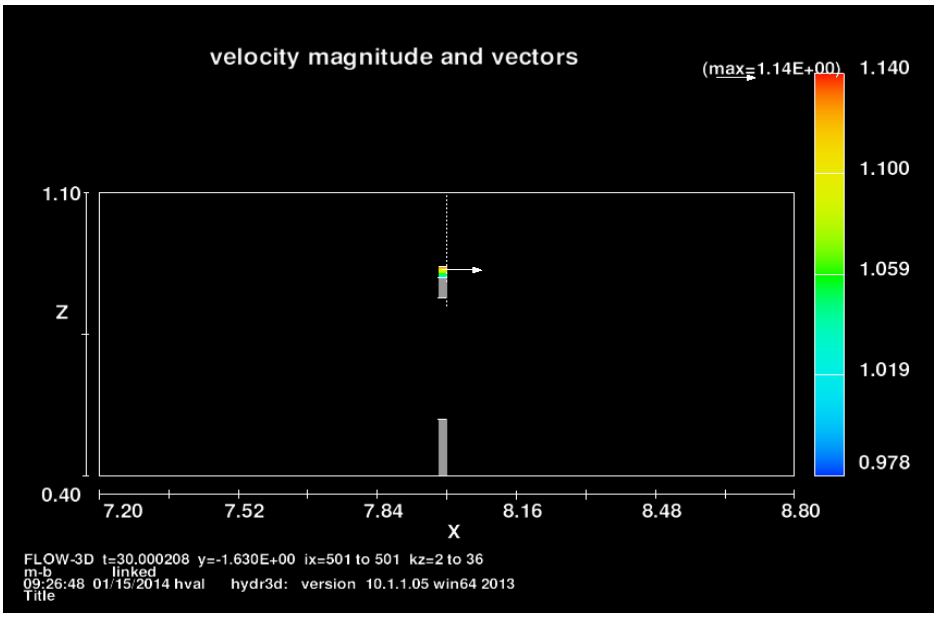

Figure A.6 Velocity profile of Fluid Particles before Grates for Q_T=0.025 m^3/sec

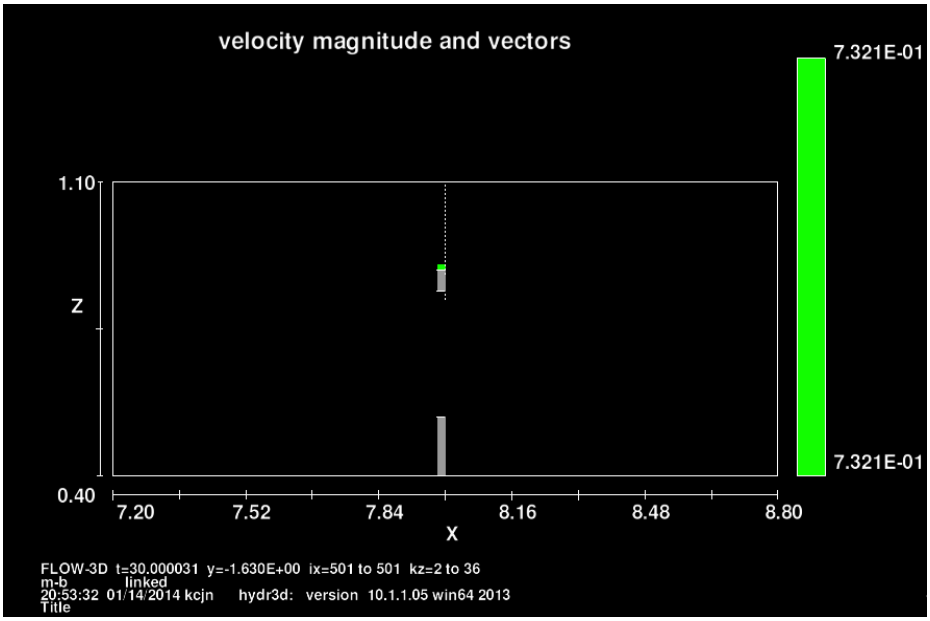

Figure A.7 Velocity profile of Fluid Particles before Grates for Q_T=0.01 m^3/sec

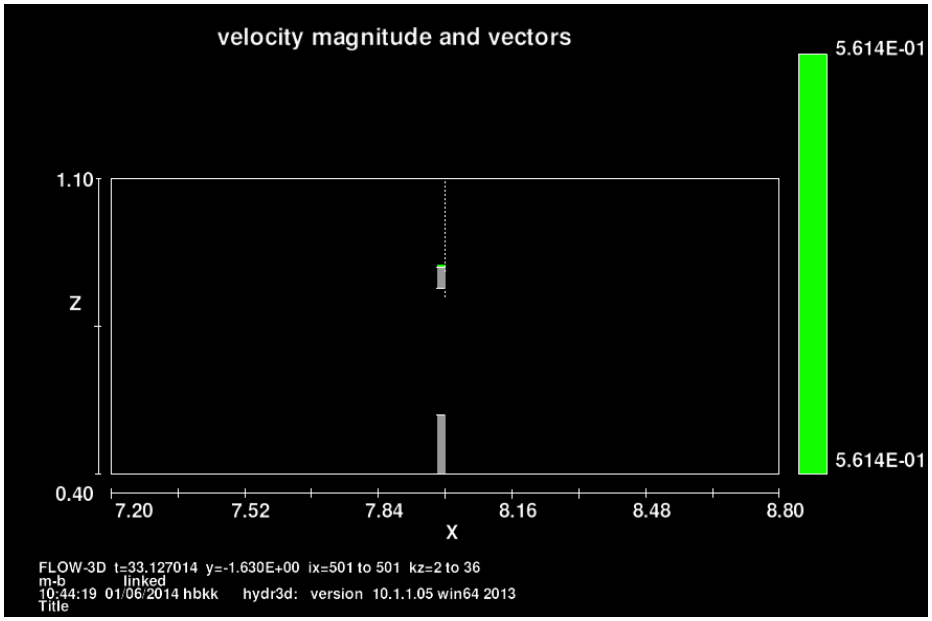

Figure A.8 Velocity profile of Fluid Particles before Grates for Q_T=0.00427 m^3/sec